Doctoral Dissertation

Pinpointed Muscle Force Control Using Power-assisting Device

Ming Ding

February 4, 2010

Department of Information Systems
Graduate School of Information Science
Nara Institute of Science and Technology

A Doctoral Dissertation
submitted to Graduate School of Information Science,
Nara Institute of Science and Technology
in partial fulfillment of the requirements for the degree of
Doctor of ENGINEERING

Ming Ding

Thesis Committee:
  Professor Tsukasa Ogasawara   (Supervisor)
  Professor Kunihiro Chihara   (Co-supervisor)
  Associate Professor Jun Takamatsu   (Co-supervisor)
  Assistant Professor Jun Ueda   (Georgia Institute of Technology)

Pinpointed Muscle Force Control Using Power-assisting Device[*]

Ming Ding

Abstract

Power-assisting system is an important research area of robotics technology for enhancing the mobility of senior citizen and people with disability. Power-assisting device uses the assist power of actuators to support operator's athletic ability (e.g. reduce load or increase ability), such as for assembly operation and outdoor work. Other potential applications are for muscle rehabilitation and sports training. Various power-assisting devices have been developed for supporting the human joint torque. Power-assisting device is also expected to support the load of muscle individually, such as for muscle function diagnostic, muscle force test and sport training. However, most of the power-assisting devices can only control the joint torque, thus making it difficult to control the muscle force due to the nonlinear and complex relations among muscles to support a particular muscle.

The purpose of this research is to propose a Pinpointed Muscle Force Control (PMFC) method to control the load of selected muscles by using power-assisting device, thus enabling pinpointed motion support, rehabilitation, and training by explicitly specifying the target muscles. By taking into account the physical interaction between human muscle forces and actuator driving forces during power-assisting, the feasibility of the muscle force desired in the PMFC method is also analyzed as a constrained optimization problem

We also developed a control system, named Muscle Assist System (MAS). It provides an easy operation to calculate and control muscle force to desired

i

value. Software configures the target muscle force and computes the driving force of power-assisting device. It is composed as modules depending on the PMFC algorithm. Graphics user interface is created, which simplifies the configuration, calculation and control of the target muscle force and driving force. Two power-assisting device, a wearable device and an unwearable device, are used as hardware to control the human force actually in experiments.

The proposed PMFC method is tested by simulation and experiments. In experiments, surface electromyographic (EMG) signals of several target and non-target muscles are measured. Two power-assisting devices are examined and the result shows the possibility of controlling the target muscle and the difference among each power-assisting device. The validity of the PMFC method is confirmed by comparing the change rates of EMG signals and the estimated muscle force in simulation.

Keywords:

パワーアシスト装具を用いたピンポイント筋力制御*

丁 明

内容梗概

高齢者や障害者の運動支援のため，パワーアシストシステムの研究は，ロボット技術における重要な研究分野の一つとなっている．パワーアシストとはアクチュエータの補助動力を用いて動作における操作者の運動能力を補助する（負荷軽減・能力増大を行う）技術である．高負荷の組立作業や野外活動の支援をはじめ，最近は福祉医療分野への応用が期待されている．アクチュエータの制御により操作者の負荷を増加させることも可能である．現在，様々なパワーアシスト装置が開発されているが，多くが関節トルクレベルでの補助を目的としている．筋肉の機能診断，筋力テストやスポーツトレーニングなどへの応用を考えたとき，パワーアシスト装置は特定の筋肉のみを補助できることも期待されている．しかし，パワーアシスト装置で直接制御できるのは関節トルクであり，特定筋肉の補助（阻害）を行うためには，複雑の筋肉間の非線形な関係を踏まえた上でパワーアシスト装具の出力を決定する必要がある．

本研究では選択された対象筋肉の負荷をパワーアシスト装置を用いて局所的に制御することを目標とするピンポイント筋力制御（Pinpointed Muscle Force Control; PMFC）手法を提案する．対象とする筋肉を明示的に決定し負荷を操作することで，筋肉の機能診断や筋肉レベルのピンポイントトレーニングを実現することを目指している．本手法は，まず計測された関節トルクから各筋肉の発揮力を推定した上で，指定した対象筋肉について設定筋力の実現可能性を筋力の最適化原理に従って判断する．可能であると判断されればそれを実現するためのパワーアシスト装置の発揮力を決定する．全ての関節トルク制御が可能である理想なパワーアシスト装置から始め，一部分の自由度しか制御できない現実な装具まで考慮し，多くのアシスト装具で実現できるピンポイント筋力制御手法を提案する．

*奈良先端科学技術大学院大学 情報科学研究科 情報システム学専攻 博士論文, NAIST-IS-DD0761033, 2010 年 2 月 4 日.

　ピンポイント筋力制御の計算と実現を簡単にするため，筋肉補助システム（Muscle Assist System; MAS）も開発する．システムはソフトウェア部とハードウェア部から構成される．ソフトウェア部は筋力制御手法の各手順に従ってモジュール化され，グラフィカルユーザインターフェースにより，目標筋力と制御力の設定，計算と制御を簡単にする．計算された制御量により，ウェアラブル装置やロボットマニピュレータなどのハードウェアを用いて，実際にピンポイント筋力制御を行う．

　提案手法を用いてシミュレーションと実機実験を行う．二つのパワーアシスト装置を用いることにより，対象筋肉が制御可能であることを示し，制御自由度が非対象筋肉に与える影響についても示す．実験中の対象筋肉に表面筋電計を取付け，人間の筋肉が活動する時に，皮膚表面から発生する表面筋電 (EMG) 信号を計測する．計測された目標筋肉の変化とシミュレーションでの推定値と比較することにより提案するピンポイント筋力制御の有効性を確認した．

キーワード

筋力制御，パワーアシスト装置，筋力推定，筋骨格モデル

Contents

List of Figures

List of Tables

List of Symbols

Chapter 1

Introduction

1.1 Background

Power-assisting device and power-assisting system are wildly researched as an important research area of robotics, to enhance the mobility of senior citizen and people with disability. Using the driving force applied by actuators, power-assisting device can support operator's athletic ability (reduce load or increase ability). The potential applications of power-assisting devices are covered from assembly operation and outdoor work to muscle rehabilitation and sports training. Various power-assisting devices have been developed for supporting human exercise capacity and the validation of these devices have been confirmed in many experiments. On the other hand, for supporting human athletic ability accurately and more effectively, many kinds of human models have also been developed to estimate the states of human body (e.g. posture, speed, force, and so on). As the background of this research, some typical power-assisting devices and human models developed in past research are introduced in the following section.

1.1.1 Power-assisting devices

Power-assisting devices are classified into wearable devices and unwearable devices. Table 1.1 shows some major characteristics of the developed power-assisting devices.

Wearable devices

Wearable power-assisting device is also called *Wearable Robot (WR)* which has a closest interaction with operator. Wearable devices are a person-oriented robots and designed to wear around operators. Generally, wearable devices can be controlled intuitively and have the same degree of freedom (DOF) of human body.

To our knowledge, the earliest research of wearable device was Yagn's *Running*

aid proposed in 1890 [1]. In his invention, two large springs operating in parallel to the legs were consisted to augment running and jumping. With the support of the power from two springs, the length of stride can be increased. Although Yagn's mechanism was proposed to support human walking and running, at last this device had not been built successfully. In 1960s, researchers at General Electric Research and the Cornell University finally succeeded in construction of *Hardiman*, a prototype full-body power-assisting device [2]. It was a huge machine with 30 hydraulic-driving DOFs and more than 680 [kg]. With the support of motor power, it can amplify the power of operator's arm and leg.

During the last two decades, with the development of robotics technology, many kinds of actuators and sensors were used to develop power-assisting devices. The most successful work in these researches has been *Berkeley Lower Extremity Exoskeleton (BLEEX)*, a exoskeleton for leg support, developed by Prof. Kazerooni's team at the University of California for Defense Advanced Research Projects Agency (DARPA) program [3, 4]. *BLEEX* was powered by internal-combustion engine and driven by hydraulic pumps. The force between human and device was measured by many sensors to control the actuators intelligently. By minimizing the human load, *BLEEX* realized a high walking and carrying capacity. Kazerooni's team also developed another 6 DOFs power-assisting device *Hydraulic Extender* for human arm assistant. This device can arbitrarily amplify the output power of operator's arm via measuring the force data of human-machine and machine-object.

Wearable Energetically Autonomous Robot (WEAR) is another power-assisting device of DARPA program, which was created by Sarcos Research Corporation [5]. Similar to *BLEEX*, the force between operator and device was measured to control the movement of device. Contrary to *BLEEX*, *WARE* was driven by rotary servomotor. It also achieved high moving and carrying capacity.

Unlike the active devices, some passive power-assisting devices also have been developed for human motion support purpose. One type of these passive devices was developed by Prof. Goldfarb's team [6]. This device was designed to assist the lower limb of spinal-cord-injury victim. Instead of active motors, brakes were used to control the joint torque of hip and knee passively.

In Japan, for the upcoming aging society, many kinds of power-assisting de-

vices have been developed. The most famous one was *Hybrid Assistive Leg (HAL)*, a full-body power assist suit, developed by Prof. Sankai's team at the University of Tsukuba [7], for performance-augmenting and rehabilitative purposes. The leg construction of *HAL* supported the flexion/extension movement at the hip and knee via DC motors. In distinction from *BLEEX* or *WEAR*, *HAL*'s system was controlled by electromyography (EMG) signals. Skin-surface EMG electrodes were placed below the hip and above the knee on both the front and the back sides of the wearer's body. Stable walking assistant has been realized using a dynamics human-device model of the human-device system. The most recent type, *HAL-5*, is a full-body assistable device and can support the full-body motion, both upper and lower limb.

Another device has been developed by the researchers at Kanagawa Institute of Technology in Japan for assisting nurses during patient transfer [8]. Pneumatic rotary actuators were used to flex/extend the hips and knees joint. In order to reduce the effect of electromagnetic noise in the hospital, a kind of muscle hardness sensor was invented to measure the contraction of human muscles. This device can determine the torque required at the joint using the muscle hardness data and the joint angle information.

Using a kind of artificial pneumatic muscles, the McKibben actuators, Prof. Noritsugu's team at Okayama University developed many kinds of power-assisting devices to assist each part of human body (e.g. leg, hip and arm) [9, 10, 11]. For example the arm assisting device they developed named *ASSIST*, can control the load in human joint via actuators and force sensors.

Prof. Kanaoka also have been developing a power-assisting device. Just like *Hydraulic Extender*, it can amplify the power of human upper limb [12]. The expansion of lower limb was also developed to support standing and walking.

Other wearable power-assisting devices developed in Japan include HONDA's *Walking Assist Device* [13] and Activelink's *Robot Suit* [14].

Unwearable devices

Unwearable power-assisting devices were mainly developed for human-machine collaborative work. The construction of most unwearable devices is not similar to human body. The movement of these devices is not controlled by the operator

directly. Most of these devices can recognize the motion or intent of the operator and use these data to decide the assist method. As a result, these devices can support the motion and reduce the load.

One famous unwearable power-assisting device has been *MIT-Manus*. It was developed by Prof. Hogan's team at Massachusetts Institute of Technology in two decades ago for rehabilitation purposes [15]. *MIT-Manus* calculates the driving force by measuring the patients' force. It is consisted of several modules. The link structure and the range of movement of the robot arm can be changed to fit for the treatment of patients. The clinical experiment in two decades proved its effectiveness in neurorehabilitation. Prof. Furuso's team also developed a similar device for rehabilitative purpose [16]. Instead of active motors, the joint torque in this device was controlled by a type of ER brake passively.

The *REHAROB* project led by Prof. Zlatov, mounted some robot arms to the human upper and lower arm for rehabilitation purpose [17]. They analyzed the basic movement of rehabilitation treatment and control the robot arms to realize it. By measuring the reaction force from operator, the movement of robot arms can be adjusted automatically. In Japan, Yaskawa Electric Corporation developed a similar power-assisting device, dubbed *TEM LX2 type D*, for automatic rehabilitation of leg [18]. *TEM* is a 2-DOF robot arm. It can conduct the movement of rehabilitation treatment automatically via the information measured by angular and force sensors.

1.1.2 Human model and application

Human model is to estimate and measure the states of human body, thus applying better human athletic ability support. For example, in the design of Perry's arm assist device or Kobayashi's *Muscle Suits*, human model is used to consider the complex link structure of human shoulder [20]. Some biomedical signals measured from human body were also used to control the power-assisting device by using the human model, for example the electromyography (EMG) signal used in *HAL* (Prof. Sankai et al.)[7] and the muscle hardness used in *Power Assist Suit* (Prof. Yamamoto et al.)[8]. For supporting human movement using a robot arm, Prof. Shibada's team proposed a method without using any force sensor [19]. The data of EMG signal and human posture was used as a virtual force sensor to estimate

Table 1.1. Power-assisting devices

Device	Assisting Part	Control signal	Power Source	Actuator
Running aid [1] (Yagn et al.)	Lower limb	-	-	Spring
Hardiman [2] (General Electric)	Full body	-	Electric	Motro
BLEEX [3, 4] (Kazerooni et al.)	Full body	Force	Hydraulic	Direct Motor
Hydraulic Extender [12] (Kazerooni et al.)	Arm	Force	Hydraulic	Motor
WEAR [5] (Sarcos)	Full body	Force	Electric	Motor
HAL [7] (Sankai et al.)	Full body	EMG	Electric	DC Motor
Power Assist Suit [19] (Yamamoto et al.)	Lower limb	Muscle hardness	Air	Artificial Muscle
Muscle Suits [20] (Kobayashi et al.)	Upper limb	-	Air	Artifical Muscle
ASSIST [11] (Noritsugu et al.)	-	-	Air	McKibben Actuator
Robot Suit [14] (Activelink)	Lower limb	Joint angle	Air	McKibben Acturator
MIT-Manus [15] (Hogan et al.)	-	Force	Electric	Motor
REHAROB [17] (Zlatov et al.)	-	-	Electric	Motor
TEM LX type D [18] (YASKAWA)	-	-	Electric	Motor

5

the output force from the human hand.

Additionally, some power-assisting research also used human internal model (e.g. musculoskeletal model, and circulatory system model) to measure or estimate internal state of human body for more accuracy support. The musculoskeletal structure has direct relation with human motion and load. It is the most necessary in power-assisting device reseach. However, the musculoskeletal structure of human body is very complex. Currently, various musculoskeletal models have been developed to estimate the movement of human muscle. The most famous models include *SIMM* (MusculoGraphics, Inc.) [21], *AnyBody* (Cybernet Systems CO. LTD.) [22], *LifeMod* (LifeModeler, Inc.) [23] and *ARMO* (GSport Inc.) [24]. The validity of these models have been confirmed from many research methods. Using these musculoskeletal models, in many power-assisting research, the load of muscle was considered for human assistant. For example, in the research of Prof. Komura at University of Edinburgh, a musculoskeletal model of arm was used to show the states of patients' body for remote rehabilitation purpose [25].

1.2 Research purpose

Currently, various power-assisting devices and assist methods have been developed. Most of these research methods focused on how to assist human motion or force in joint torque level. However, in some cases, power-assisting devices are also expected to support the muscle load individually, such as for muscle function diagnostic, muscle force test and sport training.

In this dissertation, we proposed a novel method named **Pinpointed Muscle Force Control (PMFC)**, to control the load of selected muscles by using a power-assisting device as shown in Fig. 1.1, thus enabling pinpointed motion support, rehabilitation, and training by explicitly specifying the target muscles. By taking into account the physical interaction between human muscle forces and actuator driving forces during power-assisting, the feasibility of this pinpointed muscle force control is analyzed as a constrained optimization problem.

This muscle force control is formulated as a constrained optimization problem. Driving force of power-assisting device is calculated based on minimizing problem of muscle force estimation. A mathematical analysis obtains a closed-form solution for a feasible set of desired forces for target muscles. This analysis

6
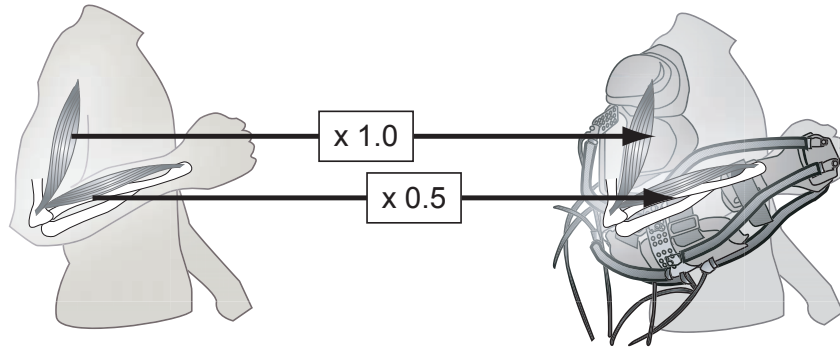
Figure 1.1. Pinpointed muscle force control

is more rigorous than the numerical iterative method.

We also developed a control system named **Muscle Assist System (MAS)** to simplify the calculation and control of PMFC. Software sets and computes the target muscle force and the driving power of device. The software is composed of some modules based on the algorithm of PMFC method. Graphical user interfaces are used in the software, thus makes it easy to configure, calculate and control the target muscle force and driving power. As the hardware, two power-assisting devices (a power-assisting suit and a robot manipulator) are used to control the human force actually.

The proposed PMFC method is tested in simulation and experiments. In simulation, the control result given by power-assisting devices shows the possibility of controlling the target muscles and the difference among each power-assisting device. In experiments, surface electromyography (EMG) signals of target and non-target muscles are measured. The validity of the PMFC method is confirmed by comparing the change rates of the EMG signals and the estimated forces.

1.3   Dissertation organization

This chapter presents the background and the main goal of this research work. It introduces the past research and explains why and where pinpointed muscle force control is necessary.

The chapter 2 introduces an overview of the pinpointed muscle force control method. It also presents some past methods of pinpointed muscle force control and the algorithm using in this research.

The chapter 3 explains the detail of the pinpointed muscle force control method proposed in this dissertation. Two calculation methods of joint torque control and external force control are derived analytically for different degree of freedom in assist device.

The chapter 4 introduces the configuration of the force assist system developed in this research. The software of the this system is modularized and designed to make setting and control easy. As hardware, two assist devices used in this research, a power-assisting suit and a robot manipulator, are presented.

The chapter 5 and 6 present the results of simulation and experiments. The results show the validity of the pinpointed muscle control method.

Finally, in Chapter 7, a conclusion terminates the dissertation by summarizing the main contributions and giving the directions of future works.

Chapter 2

Pinpointed Muscle Force Control

2.1 Summary

The purpose of Pinpointed Muscle Force Control (PMFC) proposed in this research is to control the load of a part of muscles selected by user, which has no effect on other muscle and do not change the human's posture or motion. Consider a motion assisted by a power-assisting device. Let $\boldsymbol{\tau} \in \boldsymbol{R}^M$ be a total joint torque vector needed for a target motion. At joint level, the resultant joint torque $\boldsymbol{\tau}$ is simply the sum of human torques and assist torques represented by:

$$\boldsymbol{\tau} = \boldsymbol{\tau}_h + \boldsymbol{\tau}_a, \tag{2.1}$$

where $\boldsymbol{\tau}_h \in \boldsymbol{R}^M$ is the human joint torque; $\boldsymbol{\tau}_a \in \boldsymbol{R}^M$ is the torque generated by a power-assisting device. M is the number of the control joints. Power-assisting devices are designed as the interface to apply forces or torques to the user. The torques created by the actuators are transmitted to the user's body through the joints. The joint-level effect is relatively easy to examine, by analyzing the interaction between tow rigid link mechanisms, e.g., the human body and assisting device.

However, the purpose of this research is to control the muscle force. At first, it is necessary to know how large force the human muscle extorted. In bio-informatics studies, many kinds of different ways that a muscle can generate force have been found [26]. Some of these ways are active ways worked by nervous control. However, one of these ways shows that muscle can also generate force by stretching without nerve stimulation, just like a spring. By these active and passive ways, without changing the muscle length and position, muscle can also gain various force. An example of this would be the hold motion while having different weight in hand. With contracting, muscle produces linear force. From this linear force and the moment arm about the joint's center of rotation, the rotary motion and torque of human body are produced. The function of each

Estimated nominal muscle forces

Nominal Motion

$$\sum_i \left(\frac{f_i}{PCSA_i}\right)^r \to \min$$

subject to $\quad \tau_h = A \cdot f = \tau$

x 0.5

x 0.5

$$\sum_i \left(\frac{f_i}{PCSA_i}\right)^r \to \min$$

subject to $\quad \tau_h = A \cdot f = \tau - \tau_a$

Desired muscle forces

Assisted Motion

Assist torque by Power-assisting device
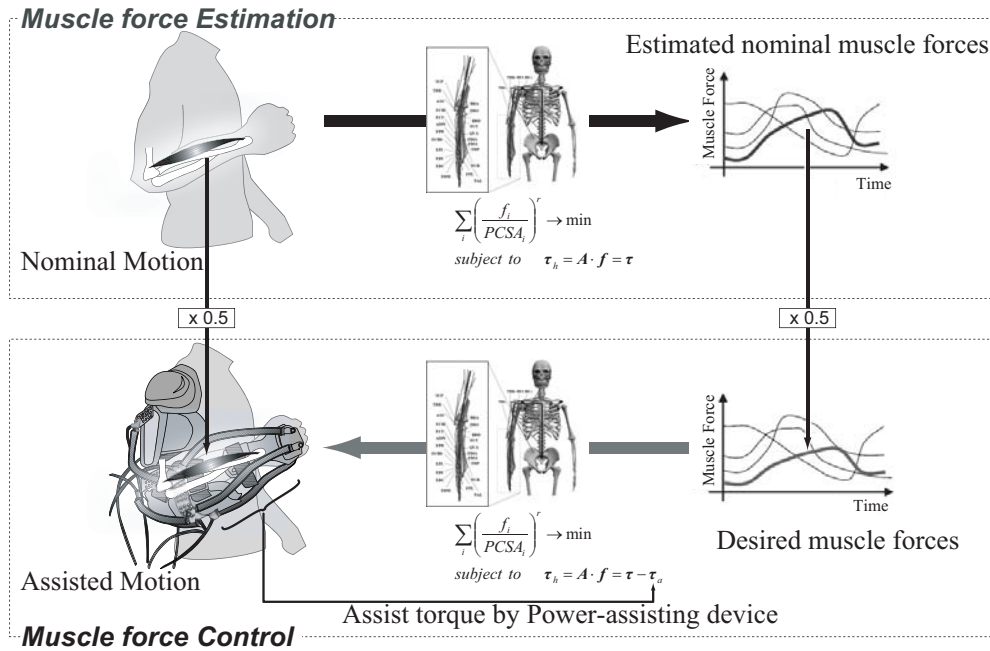
Figure 2.1. Concept of muscle force control

muscle depends on its position. For example, as the main muscles of upper arm, Biceps, Coracobrachialis and Brachialis can all work for flexing the elbow, but Biceps brachii can also work for supinating the forearm and Coracobrachialis can pronating it. All muscles product output force cooperatively and optimally [27]. So it is possible to change the distribution of muscle forces by changing the joint torque without changing the posture. The detail of this musculoskeletal model and the muscle force estimation method is explained in Appendix A.

The concept of PMFC is to control a power-assisting device such that a desired set of muscle forces is realized as illustrated in Fig. 2.1. The upper part of Fig. 2.1 illustrates the scheme where the distribution of subject's muscle forces is estimated from posture measurement. If the joint torque is controlled precisely, only a part of muscles force would be changed without effecting on other muscles. The main problem that have to be solved in this research is to obtain the joint torque and control it. The bottom part of Fig. 2.1 shows the idea of the muscle force control; the flow is basically the inverse of muscle force estimation, where desired muscle forces are given, e.g. based on nominal muscle forces without

assisting, then the joint torques that the power-assisting device generates are calculated. However, this muscle force control at the level of individual muscles is not straightforward. Excluding direct stimulation of individual muscles, the distribution of muscle forces are indirectly controlled through the modification of a limited number of joint torques by power-assisting devices.

2.2 Past control methods

In past research, two methods have been proposed to solve this problem to calculate the joint torque to realize the desired force of target muscle. One method is to simplify the human musculoskeletal model to make the calculation easy. The other one is to search the solution in iterative calculation.

2.2.1 Model simplification method

For getting the relation between muscle force and joint torques, a method to simplify the musculoskeletal model was proposed. For a detailed musculoskeletal model (e.g. the model in this research shown in Appendix A), the number of muscle forces and joint torques is too large to get the relation between their from the muscle force estimation problem defined as (2.11). However, a lot of simplified human musculoskeletal models have also been developed, and the verifications were confirmed by experiments.

Figure 2.2 shows a well-used simplified musculoskeletal model, which is proposed by Prof. Kawato [28]. Table 2.1 shows the moment arms of each muscle. In this model, using the same muscle force estimation method introduced in Appendix A.3, the muscle force can be calculated by solving following optimization problem.

$$u(f) = \sum f_j \rightarrow \min, \tag{2.2}$$

$$\text{such that:} \begin{cases} \boldsymbol{\tau}_h = \boldsymbol{A}\boldsymbol{f}; \\ f_j \geq 0 (j = 1, 2, \cdots, 6), \end{cases}$$

where $\boldsymbol{f} = [f_1, f_2, \cdots, f_6]^T$ is the muscle force vector of all 6 muscles. $\boldsymbol{\tau} = [\tau_1, \tau_2]^T$ is the joint torque vector for shoulder and elbow joint. $\boldsymbol{A}$ is the moment arm
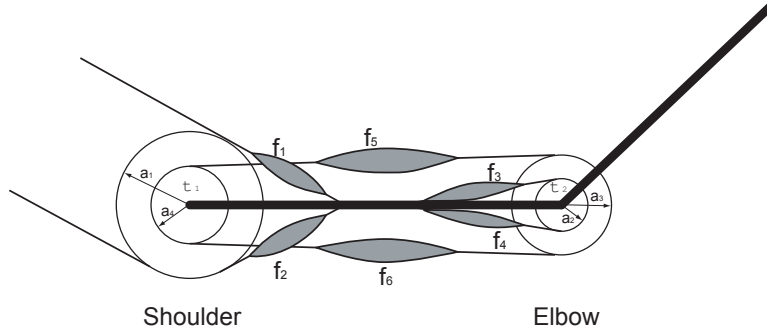
Figure 2.2. Simplified musculoskeletal model

Table 2.1. Moment arms of simplified model

	a_1	a_2	a_3	a_4
Moment arm [cm]	4.0	2.5	3.5	2.8

matrix of all muscles defined as:

$$
\begin{aligned}
A &= \begin{bmatrix} a_1 & -a_1 & 0 & 0 & a_4 & -a_4 \\ 0 & 0 & a_2 & -a_2 & a_3 & -a_3 \end{bmatrix} \\
&= \begin{bmatrix} 0.040 & -0.040 & 0 & 0 & 0.028 & -0.028 \\ 0 & 0 & 0.025 & -0.025 & 0.035 & -0.035 \end{bmatrix}.
\end{aligned}
\tag{2.3}
$$

The solution of this estimation problem is:

When $\tau_1 \geq 0$,

if $(\tau_1/\tau_2 < -0.53 \text{ or } \tau_1/\tau_2 > 0):$ else: $\tag{2.4}$

$$
\begin{cases} f_1 = 21.45\tau_1 + 11.36\tau_2 \\ f_2 = 0 \end{cases}, \qquad \begin{cases} f_1 = 0 \\ f_2 = -21.45\tau_1 - 11.36\tau_2 \end{cases}
$$

if $(-2.43 < \tau_1/\tau_2 < 0):$ else: $\tag{2.5}$

$$
\begin{cases} f_1 = -7.10\tau_1 - 17.28\tau_2 \\ f_2 = 0 \end{cases}, \qquad \begin{cases} f_1 = 0 \\ f_2 = 7.10\tau_1 + 17.28\tau_2 \end{cases}
$$

if $(\tau_1/\tau_2 < 0 \text{ or } \tau_1/\tau_2 > 3.20):$ else: $\tag{2.6}$

$$
\begin{cases} f_5 = 5.07\tau_1 - 16.23\tau_2 \\ f_6 = 0 \end{cases}, \qquad \begin{cases} f_5 = 0 \\ f_6 = -5.07\tau_1 + 16.23\tau_2; \end{cases}
$$

12

else when $\tau_1 < 0$,

$$\text{if } (-0.53 < \tau_1/\tau_2 < 0): \qquad\qquad \text{else:} \qquad\qquad\qquad (2.7)$$
$$\begin{cases} f_1 = 21.45\tau_1 + 11.36\tau_2 \\ f_2 = 0 \end{cases} , \qquad \begin{cases} f_1 = 0 \\ f_2 = -21.45\tau_1 - 11.36\tau_2 \end{cases}$$

$$\text{if } (\tau_1/\tau_2 < -2.43 \text{ or } \tau_1/\tau_2 > 0): \qquad \text{else:} \qquad\qquad\qquad (2.8)$$
$$\begin{cases} f_1 = -7.10\tau_1 - 17.28\tau_2 \\ f_2 = 0 \end{cases} , \qquad \begin{cases} f_1 = 0 \\ f_2 = 7.10\tau_1 + 17.28\tau_2 \end{cases}$$

$$\text{if } (0 < \tau_1/\tau_2 < 3.20): \qquad\qquad \text{else:} \qquad\qquad\qquad (2.9)$$
$$\begin{cases} f_5 = 5.07\tau_1 - 16.23\tau_2 \\ f_6 = 0 \end{cases} , \qquad \begin{cases} f_5 = 0 \\ f_6 = -5.07\tau_1 + 16.23\tau_2. \end{cases}$$

This solution gives all relations of muscle force and joint directly. Using this relation, target muscle force can be designed arbitrarily. However, designable muscle force and the design accuracy are limited by the simplified model.

2.2.2 Iterative calculation method

In order to be able to control more muscles force and to control the muscle force more accurately, an iterative calculation search method was proposed to calculate the joint torque from the force of target muscle which user designated [29].

As shown in Fig. 2.3, in this method, joint torques were changed in each search loop until the estimated force f_{c_j} is close to the desired force f_{t_j}. An evaluation function $v(f_{c_j})$ was used in this method to minimize the difference to target muscle force as follow:

$$v(f_{c_j}) = \frac{1}{N} \sum_{j=1}^{N} \frac{|f_{c_j} - f_{t_j}|}{f_{\max_j}} \times 100\%, \qquad\qquad (2.10)$$

where N is the number of muscles. The difference between estimated and target muscle force was regularized with the maximum muscle force $f_{\max_j}$.

In this method, detailed musculoskeletal model was used which made PMFC more accurate. However, since the number of variables (muscle forces and joint torques) is very large, it has to take a considerable long time to find out the best solution. Table 2.2 shows the computation time to the number of movable joints
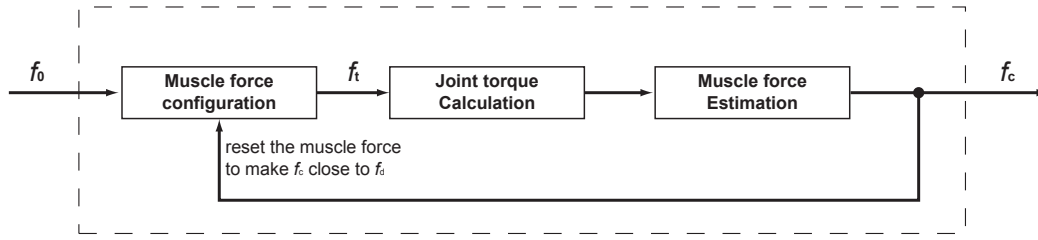
Figure 2.3. Iterative calculation search method

Table 2.2. Computation time of search method

Movable joints	1	2	3	4	5	6	7	8
Average time [s]	88.9	159.6	424.1	408.0	378.2	488.3	720.5	447.0

by using this method. If only one joint was controlled, about 1.5 minutes was needed for getting the best torque. If the number of joints was more than 3, above 7 minutes was needed to find out the solution. Therefore, this method is not practical to set and does not confirm whether the target is realizable.

2.3   Algorithm of this research

In this research, for maintaining the accuracy of muscle force control, detailed complex human musculoskeletal model is used. Instead of using the iterative calculation method, we propose a mathematical analysis method to make target muscle force design fast and accurate. A following four-step algorithm is used to control the selected muscles force arbitrarily.

Step 1 - Posture measurement: In this step, the body posture is measured and the operating load, joint angle and torque are calculated.

Step 2 - Unassisted muscle force estimation: From the human posture and the joint torque, the muscle force $\boldsymbol{f}_0$ without using the power-assisting device (i.e. $\boldsymbol{\tau}_a = 0$) is estimated by Crowninshield's method [27] defined as following muscle force estimation problem, hereafter called nominal muscle

14
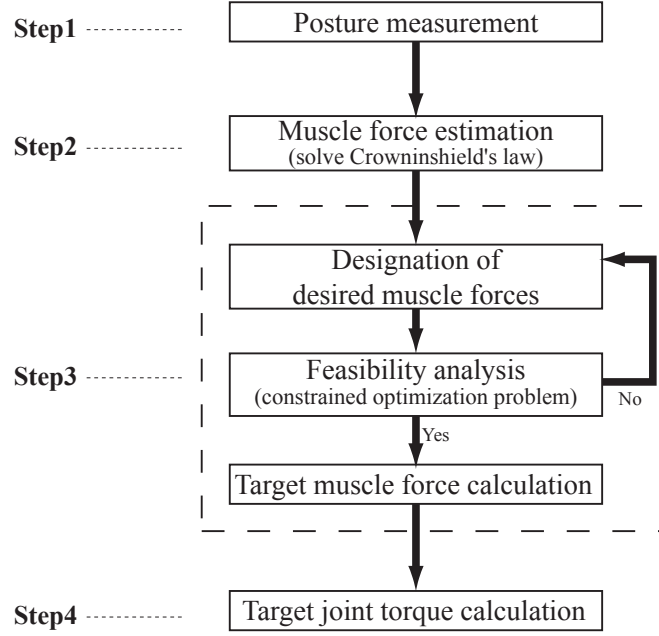
Figure 2.4. Muscle force control algorithm in this research

force.

$$u(\boldsymbol{f}) = \sum_{j=1}^{N} \left(\frac{f_j}{S_j}\right)^r \rightarrow \min, \tag{2.11}$$

$$\text{such that:} \begin{cases} \boldsymbol{\tau}_h = \boldsymbol{A}\boldsymbol{f}; \\ f_{\min j} \leq f_j \leq f_{\max j} \ _{(j=1,\cdots,N)}, \end{cases}$$

where $u(\boldsymbol{f})$ is the cost function. $\boldsymbol{A}$ is a moment arm matrix of the muscles. S_j is the physiological cross sectional area (PCSA), and $f_{\max j} = \varepsilon S_j$ is the maximum muscle force for muscle j. $\varepsilon = 0.7 \times 10^6 [\text{N/m}^2]$ was given by Karlsson [30] and S_j found in [31] are shown in Table A.1. $f_{\min j} = 0, \forall j$ is used. Also, a quadratic cost function, i.e. $r = 2$, is used for simplicity. The detail of the musculoskeletal model and the muscle force estimation method used in this research will be introduced in Appendix A.

Step 3 - Designation of desired muscle forces: Based on $\boldsymbol{f}_0$ estimated in Step 2, the desired forces of target muscle $\boldsymbol{f}_{d_t} \in \boldsymbol{R}^{N_t}$ are set by:

$$f_{dj} = \gamma_j f_{0j} \quad (j = 1, ..., N_t), \tag{2.12}$$

15

where N_t is the number of target muscle ($N_t < N$), γ_j is a rate of change for muscle j, f_{0j} is the normal muscle force of muscle j. The feasibility is checked based on constrained optimization problem. Then, if all $\boldsymbol{f}_{dj}$ are feasible, other muscle forces are designated and the desired joint torque $\boldsymbol{\tau}_h$ are calculated.

Step 4 - Control of power-assisting device: Finally, the joint torque and the driving force are calculated to compensate for a difference between $\boldsymbol{\tau}$ and $\boldsymbol{\tau}_h$.

In this research, any method and device can be used for the human posture measurement (Step 1), for example the 3D motion capture device used in this research. Therefore, the explanation of this step is omitted in this dissertation. The muscle force estimation (Step 2) used in this research is based on the Oya's model [29] and Crowninshield's method. The detail of the estimation method is described in Appendix A. How to designate the desired muscle forces (Step 3) and how to control the power-assisting device (Step 4) to realize these forces are the main problem in this research work. Next chapter will introduce the detail of these two steps.

Chapter 3

Muscle Force Control Methods

This chapter describes the detail about how to designate the desired force of target and non-target muscles, and calculate the driving force of power-assisting device. The desired muscle force $\boldsymbol{f}_d$ is designated based on the nominal muscle force $\boldsymbol{f}_0$ estimated by minimizing the cost function defined as (2.11). Two methods were proposed in this research to control the force of target muscles. At first, we consider the case where all joint torque of human body was controlled to realize the target muscle force for simplifying the designation and calculation. However most power-assisting devices can only drive a part of joints. Using the result calculated in this method would reduce the control accuracy. Next, an advanced method was proposed by taking into account of the degree of freedom (DOF) of power-assisting device to solve this problem, which does not need to control all of the human joint torques, but control a subset. Hereafter, the former is called as (1) **full-DOF control method**, and the latter is called as (2) **low-DOF control method**.

3.1 Classification of muscle force

Based on the muscle force $\boldsymbol{f}$, the N muscles are classified into two groups: **active muscles** and **inactive muscles**. The active muscles correspond to the elements having non-zero values ($f_j > 0$) in $\boldsymbol{f}$ ($\tilde{\boldsymbol{f}} \in \boldsymbol{f}$), and the inactive muscles correspond to zero elements ($f_j = 0$). Let $\tilde{N} \leq N$ be the number of the active muscles, and $N - \tilde{N}$ be the number of the inactive muscles. In our pinpointed muscle force control method, the inactive muscles are kept inactive even after control. The active muscles are further divided into two portions: **target muscles $\boldsymbol{f}_t$** and **non-target muscles $\boldsymbol{f}_n$**. If the number of target muscle is N_t and the number of non-target muscle is N_n, $N_t + N_n = \tilde{N}$. $\boldsymbol{f}_t$ is of interest for control. The desired rates of change are explicitly set by user and the power-assisting device is controlled to realize it. On the contrary, $\boldsymbol{f}_n$ is not of interest for control; the forces

of the non-target muscles may also be changed due to the physical coupling among muscles. The muscle force of $\boldsymbol{f}_n$ keep the same values, e.g., tries to minimize the changes of the force of non-target muscles.

Without the loss of generality, the order of the N muscles may be permutated according to the three groups: target, non-target, and inactive muscles, for the simplicity of description. Let $\tilde{\boldsymbol{f}} = [\boldsymbol{f}_t^T, \boldsymbol{f}_n^T]^T$. The force vector $\boldsymbol{f}$ is defined as:

$$
\boldsymbol{f} \triangleq \begin{bmatrix} \tilde{\boldsymbol{f}} \\ \hdashline \boldsymbol{0} \end{bmatrix} = \begin{bmatrix} \boldsymbol{f}_t \\ \boldsymbol{f}_n \\ \hdashline \boldsymbol{0} \end{bmatrix} \begin{array}{l} \cdots \text{ target muscles;} \\ \cdots \text{ non-target muscles;} \\ \cdots \text{ inactive muscles.} \end{array} \tag{3.1}
$$

Note that the actual values for $\boldsymbol{f}_n$ are not determined at this point. The moment arm matrix $\boldsymbol{A}$ is permutated accordingly.

$$
\boldsymbol{A}^T = \begin{bmatrix} \boldsymbol{A}_u \\ \hdashline \boldsymbol{A}_v \end{bmatrix} = \begin{bmatrix} \boldsymbol{A}_t \\ \boldsymbol{A}_n \\ \hdashline \boldsymbol{A}_v \end{bmatrix}, \tag{3.2}
$$

where $\boldsymbol{A}_u$ and $\boldsymbol{A}_v$ are the moment arm matrix of active and inactive muscles. $\boldsymbol{A}_t$ and $\boldsymbol{A}_n$ are the moment arm matrix of target and non-target muscles.

3.2 Full-DOF control method

Considered that all of joint torques of human body can be controlled individually. At first, the feasibility of desired forces of target muscle is checked. If the desired forces is feasible, the desired force of non-target muscle is designated and the driving force of power-assisting device is calculated.

3.2.1 Feasibility of muscle force control

First, the feasibility of desired forces for target muscle set by (2.12) is examined. For simplicity, the inequality conditions $f_j \leq f_{\max j}$ $(j = 1, \cdots, N)$ in muscle force estimation problem defined as (2.11) are omitted. Since the entire muscle force set is a solution of (2.11), according on Karush-Kuhn-Tucker theorem [32] [1], the

---

[1]Please read Appendix B for the detail of Karush-Kuhn-Tucker Conditions.

entire set of $\boldsymbol{f}$ must satisfy:

$$\nabla u(\boldsymbol{f}) + \sum_{i=1}^{M} \mu_i \nabla h_i(\boldsymbol{f}) + \sum_{j=1}^{N} \lambda_j + \nabla g_j(\boldsymbol{f}) = 0; \tag{3.3}$$

$$h_i(\boldsymbol{f}) = 0 \quad (i = 1, \cdots, M); \tag{3.4}$$

$$\lambda_j g_j(\boldsymbol{f}) = 0, \lambda_j \geq 0, g_j(\boldsymbol{f}) \leq 0 \ (j = 1, 2, \cdots, N), \tag{3.5}$$

where $h_i(\boldsymbol{f}) = \tau_i - \boldsymbol{a}_i^T \boldsymbol{f}$, and $g_j(\boldsymbol{f}) = -f_j$. $\boldsymbol{a}_j \in \boldsymbol{R}^N$ is a column vector of $\boldsymbol{A}$.

$$\frac{\partial u(\boldsymbol{f})}{\partial f_j} = r \left(\frac{f_j}{S_j} \right)^{r-1} \triangleq q_j; \tag{3.6}$$

$$\frac{\partial h_i(\boldsymbol{f})}{\partial f_j} = a_{ij}; \tag{3.7}$$

$$\frac{\partial g_{j_1}}{\partial f_{j_2}} = \begin{cases} -1, & j_1 = j_2; \\ 0, & j_1 \neq j_2. \end{cases} \tag{3.8}$$

Therefore, (3.3) is written as:

$$\boldsymbol{q} = w(\boldsymbol{f}) = \boldsymbol{A}^T \mu + \boldsymbol{\lambda}, \tag{3.9}$$

where $\boldsymbol{q} = [q_1, \cdots, q_N]^T$, $\boldsymbol{\mu} = [\mu_1, \cdots, \mu_M]^T$, and $\boldsymbol{\lambda} = [\lambda_1, \cdots, \lambda_N]^T$. $w(*)$ is a conversion function for $\boldsymbol{f}$ and $\boldsymbol{q}$.

$$\boldsymbol{q} = w(\boldsymbol{f}) = r \boldsymbol{S}^{-r} \boldsymbol{f}^{r-1}; \quad \boldsymbol{f} = w^{-1}(\boldsymbol{q}) = r^{-\frac{1}{r-1}} \boldsymbol{S}^{\frac{r}{r-1}} \boldsymbol{q}^{\frac{1}{r-1}}, \tag{3.10}$$

where $\boldsymbol{S}$ is a diagonal matrix consisting of the PCSAs shown in Table A.1, $\boldsymbol{S} = \mathrm{diag}([S_1, \cdots, S_N])$. When $r = 2$,

$$\boldsymbol{q} = w(\boldsymbol{f}) = 2 \boldsymbol{S}^{-2} \boldsymbol{f}; \quad \boldsymbol{f} = w^{-1}(\boldsymbol{q}) = \frac{1}{2} \boldsymbol{S}^2 \boldsymbol{q}. \tag{3.11}$$

From (3.5), $\lambda_j = 0$ if $f_j > 0$. When the number of elements of $\tilde{\boldsymbol{f}}_d$ is $\tilde{N}$, the following equation is obtained by the permutation of the rows of (3.9):

$$\begin{bmatrix} \tilde{\boldsymbol{q}} \\ \hdashline \boldsymbol{0} \end{bmatrix} = \begin{bmatrix} \boldsymbol{A}_u \\ \hdashline \boldsymbol{A}_v \end{bmatrix} \mu + \begin{bmatrix} \boldsymbol{0} \\ \hdashline \tilde{\boldsymbol{\lambda}} \end{bmatrix}, \tag{3.12}$$

where $\tilde{\boldsymbol{q}} \in \boldsymbol{R}^{\tilde{N}}$ and $\tilde{\boldsymbol{\lambda}} \in \boldsymbol{R}^{(N-\tilde{N})}$ are non-negative, $\boldsymbol{A}_u \in \boldsymbol{R}^{\tilde{N} \times M}$ and $\boldsymbol{A}_v \in \boldsymbol{R}^{(N-\tilde{N}) \times M}$. For the nominal muscle force $\boldsymbol{f}_0 (= w^{-1}(\boldsymbol{q}_0))$, (3.12) is represented as:

$$\boldsymbol{q}_0 = \boldsymbol{A}^T \boldsymbol{\mu}_0 + \boldsymbol{\lambda}_0 \rightarrow \begin{bmatrix} \tilde{\boldsymbol{q}}_0 \\ \boldsymbol{0} \end{bmatrix} = \begin{bmatrix} \boldsymbol{A}_u \\ \boldsymbol{A}_v \end{bmatrix} \boldsymbol{\mu}_0 + \begin{bmatrix} \boldsymbol{0} \\ \tilde{\boldsymbol{\lambda}}_0 \end{bmatrix}. \tag{3.13}$$

For the desired muscle force $\boldsymbol{f}_d (= w^{-1}(\boldsymbol{q}_d))$ must satisfy:

$$\boldsymbol{q}_d = \boldsymbol{A}^T \boldsymbol{\mu}_d + \boldsymbol{\lambda}_d \rightarrow \begin{bmatrix} \tilde{\boldsymbol{q}}_d \\ \boldsymbol{0} \end{bmatrix} = \begin{bmatrix} \boldsymbol{A}_u \\ \boldsymbol{A}_v \end{bmatrix} \boldsymbol{\mu}_d + \begin{bmatrix} \boldsymbol{0} \\ \tilde{\boldsymbol{\lambda}}_d \end{bmatrix}. \tag{3.14}$$

In the muscle force control method developed in this research, $\boldsymbol{f}_{dt}$ has to be realized by applying the joint torque $\boldsymbol{\tau}_a$ from the power-assisting device. For analyzing the feasibility of $\boldsymbol{f}_{dt}$, the following theorem is derived from (3.13) and (3.14).

Theorem: Feasible Desired Muscle Force

Suppose $\tilde{\boldsymbol{\lambda}}_0$ exists, and also suppose $\exists \boldsymbol{\alpha} \in \boldsymbol{R}^{\tilde{N}}$ such that:

$$\tilde{\boldsymbol{\lambda}}_0 - \boldsymbol{A}_u \boldsymbol{\alpha} > \boldsymbol{0}. \tag{3.15}$$

A feasible set of desired muscle force ($\boldsymbol{f}_d$) is represented by:

$$\tilde{\boldsymbol{q}}_d = \tilde{\boldsymbol{q}}_0 + \boldsymbol{A}_u \boldsymbol{\alpha}, \tag{3.16}$$

where $\boldsymbol{\alpha}$ is a free parameter for defining the desired muscle, hereafter called **designate coefficient**. $\boldsymbol{\alpha}$ can be chosen freely if $\tilde{\boldsymbol{\lambda}}_0$ does exist.

Proof:

It is enough to show the existence of $\boldsymbol{\mu}_d$ and $\tilde{\boldsymbol{\lambda}}_d$ that satisfy (3.16) for the proof. Let $\boldsymbol{\mu}_d = \boldsymbol{\mu}_0 + \boldsymbol{\alpha}$ and $\tilde{\boldsymbol{\lambda}}_d = \tilde{\boldsymbol{\lambda}}_0 - \boldsymbol{A}_v \boldsymbol{\alpha}$. These parameters satisfy (3.16) since

$$\begin{aligned} \begin{bmatrix} \tilde{\boldsymbol{q}}_d \\ \boldsymbol{0} \end{bmatrix} &= \begin{bmatrix} \tilde{\boldsymbol{q}}_0 + \tilde{\boldsymbol{A}} \boldsymbol{\alpha} \\ \boldsymbol{0} \end{bmatrix} \\ &= \begin{bmatrix} \tilde{\boldsymbol{A}} \\ \boldsymbol{A}_v \end{bmatrix} \boldsymbol{\mu}_0 + \begin{bmatrix} \boldsymbol{0} \\ \tilde{\boldsymbol{\lambda}}_0 \end{bmatrix} + \begin{bmatrix} \tilde{\boldsymbol{A}} \\ \boldsymbol{A}_v \end{bmatrix} \boldsymbol{\alpha} + \begin{bmatrix} \boldsymbol{0} \\ -\boldsymbol{A}_v \boldsymbol{\alpha} \end{bmatrix} \\ &= \begin{bmatrix} \tilde{\boldsymbol{A}} \\ \boldsymbol{A}_v \end{bmatrix} (\boldsymbol{\mu}_0 + \boldsymbol{\alpha}) + \begin{bmatrix} \boldsymbol{0} \\ (\tilde{\boldsymbol{\lambda}}_0 - \boldsymbol{A}_v \boldsymbol{\alpha}) \end{bmatrix}. \end{aligned} \tag{3.17}$$

20

Comparing (3.17) with the right of (3.14), $\boldsymbol{\mu}_d = \boldsymbol{\mu}_0 + \boldsymbol{\alpha}$ and $\tilde{\boldsymbol{\lambda}}_d = \tilde{\boldsymbol{\lambda}}_0 - \boldsymbol{A}_v \boldsymbol{\alpha}$. Since (3.14) also satisfies (3.9) and the inactive muscle keeps inactive after assisted, all elements of $\tilde{\boldsymbol{\lambda}}_d$ must be positive, shown as (3.15).

$\square$

In order to have non-negative values for all the elements of $\boldsymbol{f}_{dt}$ for (3.15), $\boldsymbol{f}_{dt}$ must satisfy:

$$\begin{aligned} \boldsymbol{f}_{dt} = w^{-1}(\boldsymbol{q}_{dt}) &> \boldsymbol{0} \\ \Rightarrow \boldsymbol{q}_{dt} = \boldsymbol{q}_{0t} + \boldsymbol{A}_t \boldsymbol{\alpha} &> \boldsymbol{0}, \end{aligned} \tag{3.18}$$

where $\boldsymbol{q}_{0t} = w^{-1}(\boldsymbol{f}_{0t})$ and $\boldsymbol{A}_t$ are normal force and moment arm matrix for the target muscle respectively.

In addition, in order to guarantee the existence of $\boldsymbol{\alpha}$, $\boldsymbol{f}_{dt}$ must satisfy:

$$\mathbf{rank}(\ \boldsymbol{A}_t\ ) = \mathbf{rank}(\ \begin{bmatrix} \boldsymbol{A}_t & \Delta \boldsymbol{q}_{dt} \end{bmatrix}\ ), \tag{3.19}$$

From (3.1) and (3.16), the following equation is obtained by extracting with the target muscle force and non-target muscle force.

$$\begin{aligned} \Delta \boldsymbol{q}_{dt} &= \boldsymbol{q}_{dt} - \boldsymbol{q}_{0t} &= \boldsymbol{A}_t \boldsymbol{\alpha}; \tag{3.20} \\ \Delta \boldsymbol{q}_{dn} &= \boldsymbol{q}_{dn} - \boldsymbol{q}_{0n} &= \boldsymbol{A}_n \boldsymbol{\alpha}, \tag{3.21} \end{aligned}$$

where $\boldsymbol{f}_{0n}$ ($= w^{-1}(\boldsymbol{q}_{0n})$) is the nominal force of non-target muscle. $\boldsymbol{A}_n$ is the moment arm matrix for non-target muscle. The solution $\boldsymbol{\alpha}$ for (3.20) exists if and only if (3.19) holds.

The feasibility of target muscle force $\boldsymbol{f}_{dt}$ is checked by (3.16), (3.18) and (3.19). If $\boldsymbol{\alpha}$ exists, $\boldsymbol{f}_{dt}$ is feasible. If $\boldsymbol{\alpha}$ does not exist, $\boldsymbol{f}_{dt}$ is infeasible and need to be reset. Equations (3.16), (3.18) and (3.19) are called the **feasibility conditions of the muscle force control**. Theoretically, it is impossible to control over M muscles since the degree of freedom of the muscle force control is not greater than $\mathbf{rank}(\ \boldsymbol{A}_u\ ) \leq M$. The other non-target muscle forces are not designated uniquely, due to the lack of the degrees of freedom. Note that, each of the conditions has a physiological meaning. In the PMFC method proposed in this research, if all of the conditions are not satisfied, the control of the designated target muscles for given $\boldsymbol{f}_{dt}$ is not feasible. Therefore, the change rates of the target muscle force $\boldsymbol{\gamma}$ or the choice of the target muscles must be modified.

3.2.2 Minimizing change of non-target muscle forces

If $\boldsymbol{f}_{dt}$ is feasible, the non-target muscle force $\boldsymbol{f}_{dn}$ will be designated by (3.20). All feasible sets of $\boldsymbol{\alpha}$ can be represented by:

$$\boldsymbol{\alpha} = \boldsymbol{A}_t^+ \Delta \boldsymbol{q}_{dt} + (\boldsymbol{I} - \boldsymbol{A}_t^+ \boldsymbol{A}_t)\boldsymbol{\beta}, \tag{3.22}$$

where $\boldsymbol{\beta}$ is a free parameter, which give a range of the non-target muscle forces. Equation (3.21) is written as:

$$\begin{aligned}
\Delta \boldsymbol{q}_{dn} &= \boldsymbol{q}_{dn} - \boldsymbol{q}_{0n} \\
&= \boldsymbol{A}_n \boldsymbol{\alpha} \\
&= \boldsymbol{A}_n \{\boldsymbol{A}_t^+ \Delta \boldsymbol{q}_{dt} + (\boldsymbol{I} - \boldsymbol{A}_t^+ \boldsymbol{A}_t)\boldsymbol{\beta}\} \\
&= \boldsymbol{A}_n \boldsymbol{A}_t^+ \Delta \boldsymbol{q}_{dt} + \boldsymbol{A}_n (\boldsymbol{I} - \boldsymbol{A}_t^+ \boldsymbol{A}_t)\boldsymbol{\beta} \\
&= \boldsymbol{Y} - \boldsymbol{D}\boldsymbol{\beta}, \tag{3.23}
\end{aligned}$$

where $\boldsymbol{Y} = \boldsymbol{A}_n \boldsymbol{A}_t^+ \Delta \boldsymbol{q}_{dt}$, $\boldsymbol{D} = -\boldsymbol{A}_n (\boldsymbol{I} - \boldsymbol{A}_n^+ \boldsymbol{A}_n)$. The change of the non-target muscle forces $(\Delta \boldsymbol{q}_{dn})$ is determined by the parameter $\boldsymbol{\beta}$. $\boldsymbol{f}_{dn}$ is obtained by solving following constrained linear least-squares problem (Appendix C) to minimize the change.

$$\| \Delta \boldsymbol{q}_{dn} \|^2 = \| \boldsymbol{Y} - \boldsymbol{D}\boldsymbol{\beta} \|^2 \rightarrow \min, \tag{3.24}$$

$$\text{s.t.} \quad \begin{cases} \tilde{\boldsymbol{\lambda}}_0 - \boldsymbol{A}_u \boldsymbol{\alpha} > \boldsymbol{0}; \\ f_{dnj} > 0 \quad (j = 1, \cdots, N_n), \end{cases} \tag{3.25}$$

where $\boldsymbol{f}_{dn}$ is given by:

$$\boldsymbol{f}_{dn} = w^{-1}(\boldsymbol{q}_{dn}) = w^{-1}(\boldsymbol{q}_{0n} + \Delta \boldsymbol{q}_{dn}). \tag{3.26}$$

3.2.3 Calculation of joint torque

Finally, the desired joint torque $\boldsymbol{\tau}_h$ is given by:

$$\boldsymbol{\tau}_h = \boldsymbol{A}\boldsymbol{f}_d = \begin{bmatrix} \boldsymbol{A}_u \\ \boldsymbol{A}_n \\ \boldsymbol{A}_v \end{bmatrix}^T \begin{bmatrix} \boldsymbol{f}_{dt} \\ \boldsymbol{f}_{dn} \\ \boldsymbol{0} \end{bmatrix}. \tag{3.27}$$

Then the joint torque of power-assisting device $\boldsymbol{\tau}_a$ is calculated from (2.1):

$$\boldsymbol{\tau}_a = \boldsymbol{\tau} - \boldsymbol{\tau}_h. \tag{3.28}$$

Here, the device joint torque $\boldsymbol{\tau}_a$ has the same size with human joint torque $\boldsymbol{\tau}_h$. For using this method, all of the human joint have to be controlled by a power-assisting device.

3.3 Low-DOF control method

In full-DOF control method, power-assisting device must have the same DOF as the human body to control all human joint torques. However, limited by the current technology, it is difficult to develop such power-assisting device. Most power-assisting device can only control a subset of human joint torques, for example for elbow or for wrist only. In order to realize the PMFC in these low-DOF control devices, an advanced method is proposed. The designated muscle force not only have to be feasible, but also must be able to be gained by the low-DOF control device.

This method is based on the result of the full-DOF control method explained in the previous section, but the joint torque of power-assisting device $\boldsymbol{\tau}_a$ is calculated in kinematics by taking into account the DOF of the power-assisting device. (1) At first, the relationship between human muscle force and device driving force is derived to get the the set of muscle force that can be realized by power-assisting device. (2) Then, the designate equation (3.16) and the feasibility conditions (3.16), (3.18), (3.19) is used to get the subset of muscle force by that target muscle force can be realized. (3) Finally, the optimum muscle force is decided from this subset while minimizing the effect for other non-target muscle. However, in order to make this low-DOF control method computable, the index number r in (2.11) have to be fixed to 2. Currently, other index number or other muscle force estimation method cannot be used for this method. The following subsections will give the detail of the derivation of this method.

3.3.1 Muscle force and driving force

Consider a power-assisting device, which can control only the subset of force and joint torque of human body. Let K be the DOF of device, which is lesser than

23

the number of human joint M, $K < M$. The generalized force given by the power-assisting devices is $\boldsymbol{F}_e = [\tau_1, \tau_2, \cdots, f_1, f_2, \cdots]^T \in \boldsymbol{R}^K$. $(\tau_1, \tau_2, \cdots)$ are the joint torques directly controlled by the devices; and $(f_1, f_2, \cdots)$ are the forces from the devices. Note that control with more than one device is forbidden in this method. Using $\boldsymbol{F}_e$ and its Jacobean matrix $\boldsymbol{J}_e \in \boldsymbol{R}^{K \times M}$, $\boldsymbol{\tau}_a$ is calculated in kinematic as:

$$\boldsymbol{\tau}_a = \boldsymbol{J}_e^T \boldsymbol{F}_e. \tag{3.29}$$

The human joint torque $\boldsymbol{\tau}_h$ is controlled by power-assisting device. From (2.1), the first constraint condition of (2.11) can be represented as:

$$\begin{aligned} \boldsymbol{\tau}_h &= \boldsymbol{A}\boldsymbol{f} \\ &= \boldsymbol{\tau}_0 + \boldsymbol{\tau}_a = \boldsymbol{\tau}_0 + \boldsymbol{J}_e^T \boldsymbol{F}_e. \end{aligned} \tag{3.30}$$

Using (3.30) as a new constraint condition in muscle force estimation problem (2.11), the muscle force $\boldsymbol{f}$ can be estimated from device power $\boldsymbol{F}_e$ directly, without using the joint torque $\boldsymbol{\tau}_a$.

However $\boldsymbol{\tau}_h$ has a different size of $\boldsymbol{F}_e$ due to $K < M$. The same method in full-DOF control can not be used to designate the target muscle force because the muscle force with assist $\boldsymbol{f}_d$ is limited by $\boldsymbol{F}_e$. The relationship between human muscle force $\boldsymbol{f}_d$ and device driving force $\boldsymbol{F}_e$ have to be derived first.

3.3.2 Feasible muscle force

Consider two feasible muscle force with and without assist, $\boldsymbol{f}_0$ and $\boldsymbol{f}_d$. $\boldsymbol{q}_0 = w(\boldsymbol{f}_0)$ and $\boldsymbol{q}_d = w(\boldsymbol{f}_d)$. If these two sets of muscle force are feasible, the change of $\boldsymbol{q}$ with and without assist can be calculated form (3.16) as:

$$\Delta \boldsymbol{q} = \boldsymbol{q}_d - \boldsymbol{q}_0 = \boldsymbol{A}^T \boldsymbol{\alpha}. \tag{3.31}$$

Therefore, the change of muscle force is:

$$\Delta \boldsymbol{f} = w^{-1}(\Delta \boldsymbol{q}) = \frac{1}{2} \boldsymbol{S}^2 \boldsymbol{q} = \frac{1}{2} \boldsymbol{S}^2 \boldsymbol{A}^T \boldsymbol{\alpha}. \tag{3.32}$$

The index number r of muscle force estimation problem (2.11) is fixed to 2 here for keeping the linear relation between $\boldsymbol{f}$ and $\boldsymbol{q}$. This change of muscle force $\Delta \boldsymbol{f}$ is applied by power-assisting device.

$$\boldsymbol{A}\Delta \boldsymbol{f} = \boldsymbol{\tau}_d - \boldsymbol{\tau}_0 = \boldsymbol{J}_e^T \boldsymbol{F}_e. \tag{3.33}$$

24

Substitute (3.32) into this equation and the designate coefficient $\boldsymbol{\alpha}$ can be rewritten in $\boldsymbol{F}_e$ as follow:

$$\begin{aligned} \boldsymbol{A}(\frac{1}{2}\boldsymbol{S}^2\boldsymbol{A}^T\boldsymbol{\alpha}) &= \boldsymbol{J}_e^T\boldsymbol{F}_e \\ [\frac{1}{2}\boldsymbol{A}\boldsymbol{S}^2\boldsymbol{A}^T]\boldsymbol{\alpha} &= \boldsymbol{J}_e^T\boldsymbol{F}_e \\ \Rightarrow \boldsymbol{\alpha} &= [\frac{1}{2}\boldsymbol{A}\boldsymbol{S}^2\boldsymbol{A}^T]^{-1}\boldsymbol{J}_e^T\boldsymbol{F}_e; \end{aligned} \tag{3.34}$$

where $\boldsymbol{A}$ is a $M \times N$ matrix, $\boldsymbol{S}^2$ is a $N \times N$ matrix and $(\boldsymbol{A}\boldsymbol{S}^2\boldsymbol{A}^T)$ is a $M \times M$ matrix.

$$\begin{aligned} \mathbf{rank}(\ \boldsymbol{A}\ ) &= M, \mathbf{rank}(\ \boldsymbol{S}^2\ ) = N, M < N \\ \Rightarrow \ \mathbf{rank}(\ \boldsymbol{A}\boldsymbol{S}^2\boldsymbol{A}^T\ ) &= \min\left(\mathbf{rank}(\ \boldsymbol{A}\ ), \mathbf{rank}(\ \boldsymbol{S}^2\ ), \mathbf{rank}(\ \boldsymbol{A}^T\ )\right) \\ &= M. \end{aligned} \tag{3.35}$$

Therefore $(\boldsymbol{A}\boldsymbol{S}^2\boldsymbol{A}^T)$ is a full rank and the inverse matrix is exist.

Substitute it into (3.31) again, $\Delta\boldsymbol{q}$ can also be obtained from the driving force $\boldsymbol{F}_e$ of power-assisting device as follow:

$$\Delta\boldsymbol{q} = \boldsymbol{A}^T\boldsymbol{\alpha} = \boldsymbol{A}^T \cdot [\frac{1}{2}\boldsymbol{A}\boldsymbol{S}^2\boldsymbol{A}^T]^{-1}\boldsymbol{J}_e^T\boldsymbol{F}_e. \tag{3.36}$$

$\Delta\boldsymbol{q}$ can be divided into $\Delta\boldsymbol{q}_t$ and $\Delta\boldsymbol{q}_n$ according to the target and non-target muscle as:

$$\Delta\boldsymbol{q}_t = \boldsymbol{A}_t \cdot [\frac{1}{2}\boldsymbol{A}\boldsymbol{S}^2\boldsymbol{A}^T]^{-1}\boldsymbol{J}_e^T\boldsymbol{F}_e = \boldsymbol{G}_t\boldsymbol{F}_e; \tag{3.37}$$

$$\Delta\boldsymbol{q}_n = \boldsymbol{A}_n \cdot [\frac{1}{2}\boldsymbol{A}\boldsymbol{S}^2\boldsymbol{A}^T]^{-1}\boldsymbol{J}_e^T\boldsymbol{F}_e = \boldsymbol{G}_n\boldsymbol{F}_e. \tag{3.38}$$

where $\boldsymbol{G}_t = \boldsymbol{A}_t[\frac{1}{2}\boldsymbol{A}\boldsymbol{S}^2\boldsymbol{A}^T]^{-1}\boldsymbol{J}_e^T$ and $\boldsymbol{G}_n = \boldsymbol{A}_n[\frac{1}{2}\boldsymbol{A}\boldsymbol{S}^2\boldsymbol{A}^T]^{-1}\boldsymbol{J}_e^T$.

3.3.3   Minimizing changes of non-target muscle force

$\Delta\boldsymbol{q}_t$ is known value for target muscle $(\Delta\boldsymbol{q}_t = w(\Delta\boldsymbol{f}_t))$, which was set in (2.12). Therefore, the generalized force of power-assisting device $\boldsymbol{F}_e$ can be determined by $\Delta\boldsymbol{q}_t$ as follow:

$$\boldsymbol{F}_e = \boldsymbol{G}_t^+ \cdot \Delta\boldsymbol{q}_t + (\boldsymbol{I} - \boldsymbol{G}_t^+\boldsymbol{G}_t)\hat{\boldsymbol{\beta}}, \tag{3.39}$$

where $\hat{\boldsymbol{\beta}}$ is a free parameter which give a range of the non-target muscle realized by the driving force $\boldsymbol{F}_e$. Substitute it into (3.38), the change of non-target muscle force $\Delta\boldsymbol{q}_n \ (= w(\Delta\boldsymbol{f}_n))$ can be represented as:

$$\begin{aligned} \Delta\boldsymbol{q}_n &= \boldsymbol{G}_n\boldsymbol{F}_e \\ &= \boldsymbol{G}_n\boldsymbol{G}_t^+ \cdot \Delta\boldsymbol{q}_t + \boldsymbol{G}_n(\boldsymbol{I} - \boldsymbol{G}_t^+\boldsymbol{G}_t)\hat{\boldsymbol{\beta}}. \end{aligned} \tag{3.40}$$

Rewrite (3.40) with $\boldsymbol{f}_t$ and $\boldsymbol{f}_n$, and the change of $\boldsymbol{f}_n$ can be given by $\boldsymbol{f}_t$ as following designate equation.

$$\Delta\boldsymbol{f}_n = \hat{\boldsymbol{Y}} \cdot \Delta\boldsymbol{f}_t - \hat{\boldsymbol{D}}\hat{\boldsymbol{\beta}}, \tag{3.41}$$

$$\begin{cases} \hat{\boldsymbol{Y}} = \boldsymbol{S}^2\boldsymbol{A}_n[\frac{1}{2}\boldsymbol{A}\boldsymbol{S}^2\boldsymbol{A}^T]^{-1}\boldsymbol{J}_e^T\boldsymbol{A}_t[\frac{1}{2}\boldsymbol{A}\boldsymbol{S}^2\boldsymbol{A}^T]^{-1}\boldsymbol{J}_e^{T+}\boldsymbol{S}^{-2}; \\ \hat{\boldsymbol{D}} = -\frac{1}{2}\boldsymbol{S}^2\boldsymbol{A}_n[\frac{1}{2}\boldsymbol{A}\boldsymbol{S}^2\boldsymbol{A}^T]^{-1}\boldsymbol{J}_e^T \\ \qquad (I - \boldsymbol{A}_t[\frac{1}{2}\boldsymbol{A}\boldsymbol{S}^2\boldsymbol{A}^T]^{-1}\boldsymbol{J}_e^{T+}\boldsymbol{A}_t[\frac{1}{2}\boldsymbol{A}\boldsymbol{S}^2\boldsymbol{A}^T]^{-1}\boldsymbol{J}_e^T). \end{cases}$$

The non-target muscle force $\boldsymbol{f}_{dn}$ is calculated by minimizing this change. The similar method of (3.24) is used by solving a constrained linear least-squares problem. The feasibility conditions for (3.34) used in full-DOF control method (3.16), (3.18) and (3.19) is also applied in this method for $\boldsymbol{f}_{dt}$. These feasibility conditions are defined as follow, which are rewritten by the known nominal muscle force $\boldsymbol{f}_0$ and desired force of target muscle $\Delta\boldsymbol{f}_t \ (= (\gamma - 1)\boldsymbol{f}_{0t})$.

1. The resultant muscle force of the non-target muscles remain positive if

$$\boldsymbol{f}_{n0} + \Delta\boldsymbol{f}_n > 0; \tag{3.42}$$

2. $\boldsymbol{f}_{dt}$ for the target muscles is completely realized if

$$\mathbf{rank}(\ \boldsymbol{A}_t\ ) = \mathbf{rank}(\ \begin{bmatrix} \boldsymbol{A}_t & (2\boldsymbol{S}^{-2}\Delta\boldsymbol{f}_t) \end{bmatrix}\ ); \tag{3.43}$$

3. The inactive muscles keep inactive if

$$\boldsymbol{A}_v \begin{bmatrix} \boldsymbol{A}_t \\ \boldsymbol{A}_n \end{bmatrix} \begin{bmatrix} \boldsymbol{S}^{-2}\Delta\boldsymbol{f}_{0t} \\ \boldsymbol{S}^{-2}\Delta\boldsymbol{f}_{0n} \end{bmatrix} \boldsymbol{A}_v\boldsymbol{S}^2\Delta\boldsymbol{f}_n < 0. \tag{3.44}$$

Proof of the designate equation (3.41) and the conditions (3.42)-(3.44) is can be done by the similar method of full-DOF control (3.17).

26

3.3.4 Calculation of driving force

Using the designated $\Delta \boldsymbol{f} = [\Delta \boldsymbol{f}_t^T, \Delta \boldsymbol{f}_n^T, \boldsymbol{0}^T]^T$, driving-force of power-assisting device $\boldsymbol{F}_e$ can be calculated from (3.32) as follow:

$$
\begin{aligned}
\boldsymbol{F}_e &= \boldsymbol{J}_e^{T^+} \boldsymbol{A} \Delta \boldsymbol{f} \\
&= \boldsymbol{J}_e^{T^+} \boldsymbol{A} \begin{bmatrix} \Delta \boldsymbol{f}_t \\ \Delta \boldsymbol{f}_n \\ \boldsymbol{0} \end{bmatrix} .
\end{aligned}
\tag{3.45}
$$

Unlike the full-DOF control method that in this low-DOF control method, any device can be used to realize the target muscle force $\boldsymbol{f}$, even though the power-assisting device can not control the the human joint torques absolutely.

Chapter 4

Muscle Force Control System

We also developed a system named Muscle Assist System (MAS) to control muscle force using PMFC method we developed. This Chapter introduces the configuration of the software and hardware used in this research.

4.1 Software

Control software calculates and controls the driving force of power-assisting device using the posture and the load measured from the human body. It also simulates the pinpointed muscle force control. The configuration of software is shown in Fig. 4.1. Depending on the muscle force control algorithm introduced in section 2.3, this software is also composed of four modules: the posture measurement module, the muscle force estimation module, the muscle force designation module and the device control module.

Posture measurement module

Any motion capture device may be used in the PMFC method. As an example, Mac3D system (NAC Image Technology, Inc.), a motion capture device, is used to measure the body posture in this research. Measurement software (EvaRT) reproduces the posture of the subject as 3 dimensional positions of the markers attached on the subject and calculates joint angles.

Muscle force estimation module

Joint torques are calculated by substituting the obtained joint data for a musculoskeletal human model described in Appendix A. This skeletal model provides the moment arms and lengths of muscles, then Crowninshield's method[27] is used to estimate the nominal muscle forces for the given posture. This estimation is solved by a quadratic programming written in C. The estimation speed is about
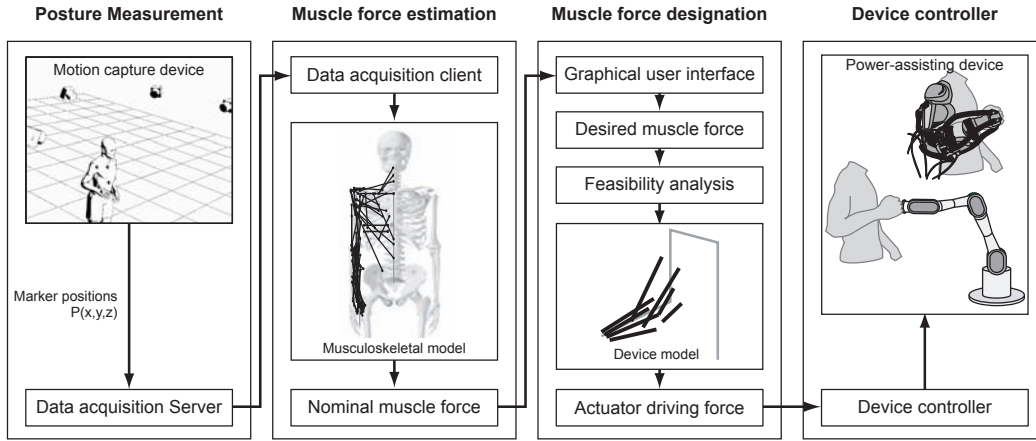
28

Posture Measurement	Muscle force estimation	Muscle force designation	Device controller
Motion capture device	Data acquisition client	Graphical user interface	Power-assisting device
		Desired muscle force	
		Feasibility analysis	
Marker positions P(x,y,z)	Musculoskeletal model	Device model	
Data acquisition Server	Nominal muscle force	Actuator driving force	Device controller

Figure 4.1. Configuration of muscle force control system

200[Hz]. This obtained muscle forces are used for the designation of muscle force in the following module.

Muscle force designation module

The target muscle force is set by given the rates of change for target muscles $\boldsymbol{\gamma}_t$ using a graphical user interface. Before designating the desired force of non-target muscle $\boldsymbol{f}_{dn}$, the feasibility of this desired force of target muscle $\boldsymbol{f}_{dt}$ is checked using the method described in Chapter 3. If the given set of $\boldsymbol{f}_{dt}$ is feasible, the non-target muscle force $\boldsymbol{f}_{dn}$ is calculated by solving a least-squares linear optimization problem using the method explained in Appendix C.2.

Device control module

This module calculates driving-force of the power-assisting devices from the designated muscle force $\boldsymbol{f}_d$. Power-assisting devices are control in feedback method. The measured data (e.g. force, position) from sensors equipped on the devices is used to calculate the control value via PID controller. When the number of actuators is larger than the DOF of power-assisting device, optimization calculation is also used for obtaining the best force set of actuators.
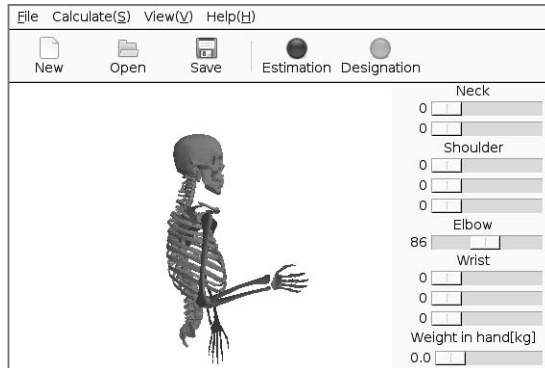
(a) Main window

(b) Result window

(c) Setting window

Figure 4.2. User interface of MAS

4.1.1 User interface

Figure 4.2(a) shows the main control window of this software. The body posture measured by posture measurement module is displayed in this window using 3D CG model in real-time. The result of the muscle force estimation is displayed in a graph. Figure 4.2b shows the result window.

The body posture can also be set off-line by changing the joint angles using slide bars. The muscle force in the posture set by a user can also be calculated. The design dialog window shown as Fig. 4.2(c) is used to set the rate of change γ. The result of muscle designation can also be displayed as a graph in the result window. Finally, it controls the device to obtain the driving-force calculated by the device control module.

4.2 Hardware

In this research, two power-assisting devices are used to confirm the validity of the method, a wearable device (a power-assisting suit) and an unwearable device (a robot manipulator). Note that, based on the pinpointed muscle force control method proposed in Chapter 3, other power-assisting devices can also be used to control the muscle force.

4.2.1 Wearable device

In order to control the muscle forces of human right upper limb, a wearable power-assisting suit shown in Fig. 4.3(a) has been developed. 8 McKibben pneumatic actuators are used in this device to apply 4 degrees of freedom (DOFs) torques of the right arm, 1-DOF of the elbow joint and 3-DOF of the wrist joint. Both ends of each actuator are attached to plastic frames which are then attached to the body by velcro tapes. Although this paper refers this robotic device as "exoskeleton," this device, unlike other exoskeleton mechanisms, does not have any rigid frames but flexible pneumatic actuators for safety reasons.

The pneumatic actuator shown in Fig. 4.3(c) with 20 [mm] diameter, maximum pressure of 0.4 [MPa], and maximum force of 60 [N] is used. This actuator contracts when pressurized by a compressor controlled by an electropneumatic regulator. The actuators are also modeled as wires and integrated with the human

(a) Device

(b) Device model
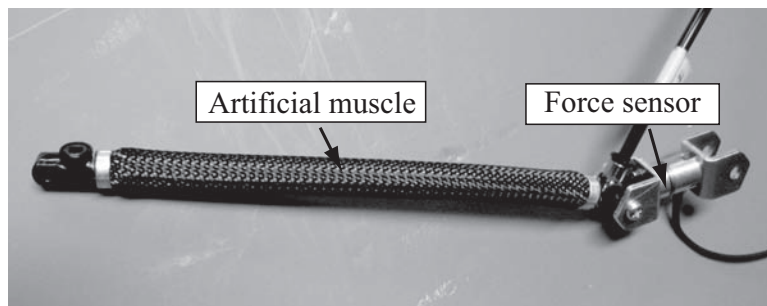
(c) Artificial muscle and force sensor

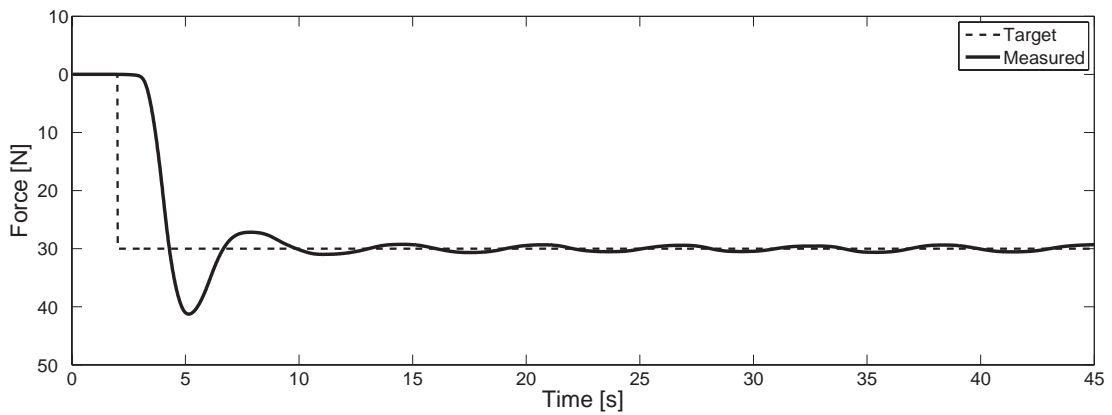Figure 4.3. Power-assisting device

Figure 4.4. Force control test of pneumatic actuator

kinematic model as shown in Fig. 4.3(b). The force of each actuator is controlled by feedback (Proportional-Integral(PI) force feedback) control using a force sensor. Force feedback control compensates for un-modeled nonlinear and dynamic characteristics of the actuator. Figure 4.4 shows the response for a stair-case reference.

4.2.2　Unwearable device

As an unwearable device, a 7-DOF robot manipulator (*PA10*, Mitsubishi Heavy Industries) shown in Fig. 4.5 is used to control the muscle forces of the human right upper limb. The tip of the manipulator can be transferred to all 3 directions and rotated on all 3 axes. A handle is designed and mounted into the tip of the manipulator in order to grasp it easily. A force sensor is set into the centre of this handle to control 3 axes force in user's hand. Origins of both handle and force sensor are aligned. It makes the measurement of the external force easy and accuracy. Appendix E will show the construction of this handle.

Limited by the measuring range of the force sensor used in the handle, maximum force of each axial applied by this robot manipulator is given as 5 [kgf] ($\approx$ 49.05 [N]). Feedback control is also used to realize the designated external force. Figure 4.6 shows the control result of the force feedback control for a downward 30.0 [N] force. The dashed line shows target force; the solid line shows the controlled force. In the stable period (e.g. 6-18 [s]), the control error was smaller than 0.22 [N] and the control accuracy is high enough for human force control.

Contrary the power-assisting suit, this robot manipulator can apply large range of movement and great output power. The control software limits the movement and the output power to prevent runaway and dangerous for subjects. In order to keep subjects safe, not only operator but also subject can stop the system immediately when they sense any dangerous by using two parallel series emergency stop switches. [1]

---

[1]The safeness of the device has been approved by Ethics Committee of NAIST.
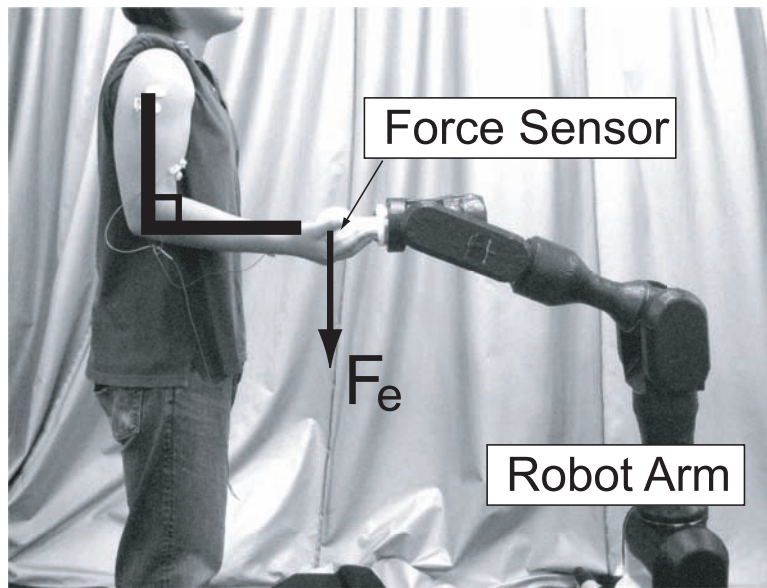
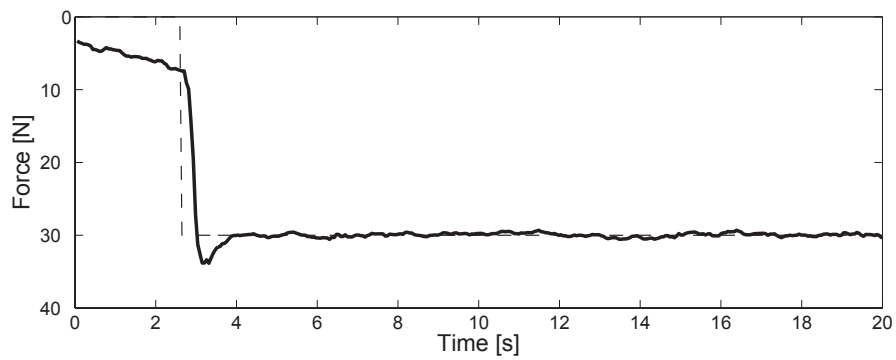Figure 4.5. Robot manipulator

Figure 4.6. Force control test of robot manipulator

Chapter 5

Muscle Force Control Simulation

This chapter describes the results of muscle force control simulation. The human posture (the angles of every joint) and the operating load are set to simulation at first. Then the force change rate of target muscle $\boldsymbol{\gamma}_t$ is set to calculate the desired muscle force. If the muscle force is feasibility, the driving torque/force would be calculated. The control possibility of target muscle will be analyzed and the change of driving torque/force will be verified.

The PMFC method proposed in this research can be used to control any posture. As an example, a posture shown in Fig. 5.1(a) is considered where the elbow joint angle is 90[deg]. An nominal external downward force $F = 10$[N] is applied to the hand. Figure 5.1(b) shows the nominal muscle forces $\boldsymbol{f}_0$ for this designated posture and external force, where the horizontal axis of the graph represents the number of muscles shown in Table A.1.

In this chapter, for testing the validity of PMFC, the following two cases are examined: (1) control of a single muscle force and (2) simultaneous control of multiple muscle forces. Then, (3) some power-assisting devices with different DOF of control are examined to analyze the effect of non-target muscle.

5.1 Control of single muscle

Feasibe case

As an example, Brachialis (BRA., No.27) is considered as a target muscle in this test. The desired muscle force for Brachialis is given as a half of the nominal muscle force, i.e. $f_{d27} = 0.5 \times f_{027}$. Using the remaining DOFs of control, other muscle forces are controlled to minimize the variation of change. Figure 5.2(a) shows the incremental rate of change of the controlled muscle forces from the nominal muscle forces. If a nominal muscle force and the controlled muscle force are the same, this graph shows 100%. Similarly, this graph shows 50% if a controlled muscle force is a half of the nominal muscle force. Black boxes represent the target mus-
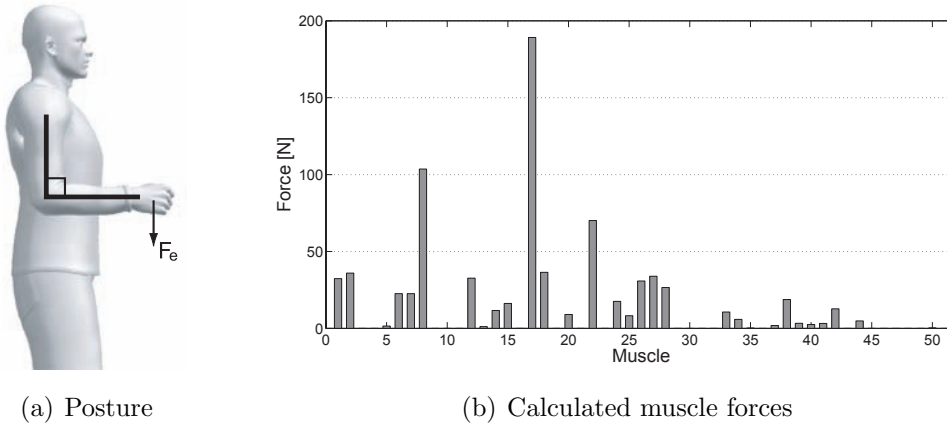
(a) Posture

(b) Calculated muscle forces

Figure 5.1. Posture for simulation and simulation result

(a) Change rate of muscle force

(b) Change of joint torque

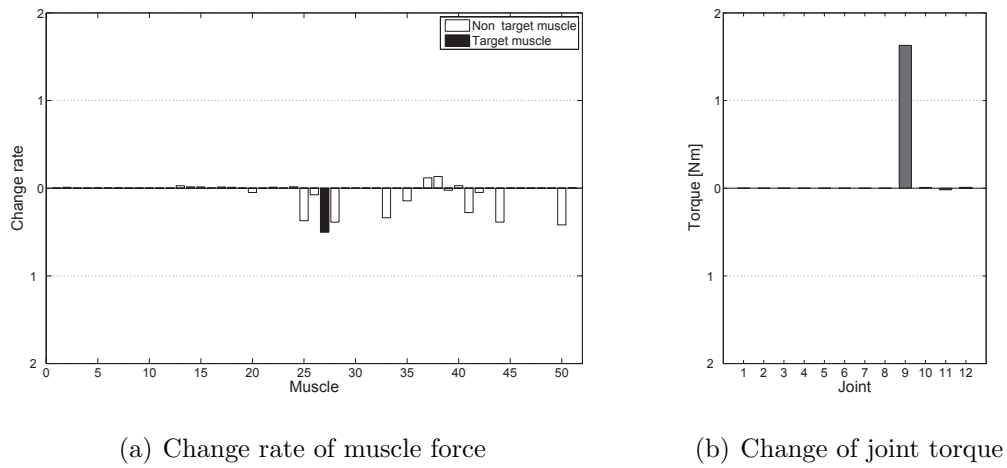Figure 5.2. Simulation result of single control
BRA. (No.27) ×0.5

cles and white boxes represent the non-target muscles. The anatomical function of Brachialis is flexion/extension of the elbow. This implies that a certain group of muscles having the similar function for the elbow may change in consequence of the control of Brachialis. As shown in the figure, Brachialis changed accordingly, showing -0.5. However, other non-target muscles also changed due to the coupling among muscles although this effect has been reduced minimally.

Figure 5.2(a) shows the change of joint torque before and after assist, that is the joint torque of power-assisting device $\boldsymbol{\tau}_a$. The horizontal axis represents the number of human joint shown in Fig. A.1(b). The result shows that in order to control the target muscle force, the joint driven by the target muscle have to be controlled.

Impossibe case

Every muscle can be controlled in a certain range of change rate if it is not inactive muscle and the nominal force of this muscle is not zero. However, if the change rate γ is too large, it will be deemed impossible by the feasibility condition (3.16) or (3.44) due to effecting the inactive muscle.

As an example, if we set the rate of change for Brachialis (BRA., No.27) to 3 times of nominal muscle force, i.e. $\gamma_{27} = 3.0$. Since the γ_{27} is too large to satisfy the feasibility condition, this change rate can not be realized in the simulation. However, even if this case was deemed impossible by checking the feasibility conditions proposed in this research, it may also be realized in other method, e.g. using the iterative calculation search method introduced in Section 2.2.2.

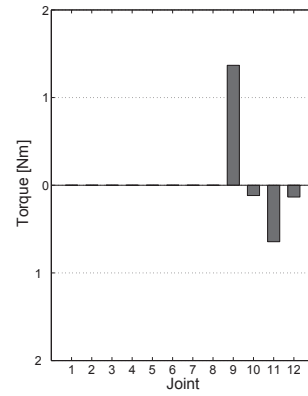## 5.2   Control of multiple muscle

Feasibe case

Figure 5.3(a) and 5.4(a) show the results when multiple muscle forces are controlled simultaneously.

In the former example, desired force of Brachialis (BRA., No.27) and Flexor Carpi Ulnaris (FCU., No.33) were given as $0.5 \times f_{027}$ and $1.5 \times f_{033}$, respectively. Brachialis is for moving the elbow, and Extensor Carpi Ulnaris is for moving the wrist. This simultaneous control is challenging, since Brachialis is supported
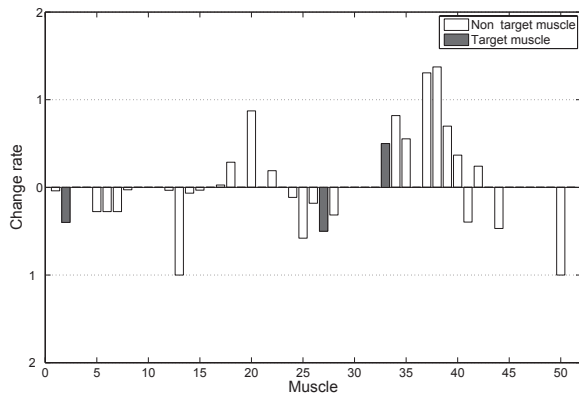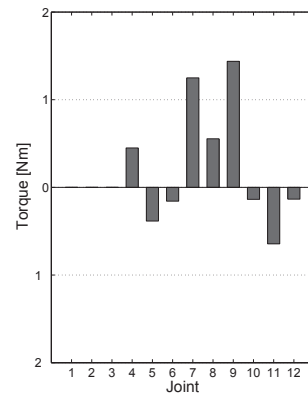
37
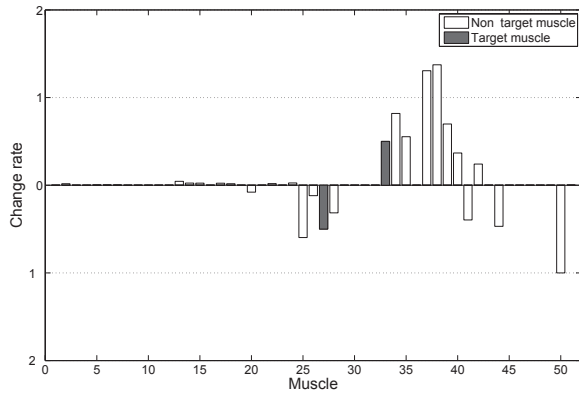
(a) Change rate of muscle force

(b) Change of joint torque

Figure 5.3. Simulation result of multiple control (I)
BRA. (No.27) ×0.5, FCU. (No.33) ×1.5

(a) Change rate of muscle force

(b) Change of joint torque

Figure 5.4. Simulation result of multiple control (II)
PEC. (No.2) ×0.6, BRA. (No.27) ×0.5, FCU. (No.33) ×1.5

but Flexor Carpi Ulnaris is trained by increasing the load. The result shows that two target muscles were controlled independently, showing -0.5 and 0.5. Similarly, other non-target muscles also changed due to the coupling among these two muscles. Figure 5.3(b) shows the change of joint torque before and after assist for this control. Main control is applied at elbow joint and wrist joint, which is similar to the function of target muscles.

In the latter example, desired force of Pectoralis (PEC., No.2) was added for $0.6 \times f_{02}$ and three muscles are control simultaneously. The anatomical function of Pectoralis is flexion/extension of the hummers. It is different from other two muscles and the result shows that this target muscle was controlled individually. Comparing with the former result, the force of other non-target coupling with this muscles are also changed. Figure 5.4(b) shows the change of joint torque before and after assist. With the increase of target muscle, more joint have to be controlled.

Impossibility case

With the exception of impossible case of single muscle control, in multiple control, it is also impossible if the target muscles are coupling to each other.

For example, consider Brachialis (BRA., No.27) and Brachioradials (BRD., No.28) as two target muscle. The function of these two muscles is to flex the elbow joint. It is very similar, thus these two muscles are strongly coupled. Therefore, the same desired rate of change should be given to them. So these two muscles cannot be controlled with a large different of change rate at once, for example giving the desired as $0.5 \times f_{027}$ and $1.5 \times f_{028}$.

5.3 Effect from DOF of power-assisting device

The Effect from the DOF of power-assisting device was tested to confirm the validity of method proposed in Section 3.3. As an example, four power-assisting devices with different DOF are examined to investigate the controllability of target muscle and the effect of non-target muscle. Each device can support a subset of 10 DOFs of human upper right body: 7 DOFs are joint torque of arm and 3 DOFs are tip force in human hand.
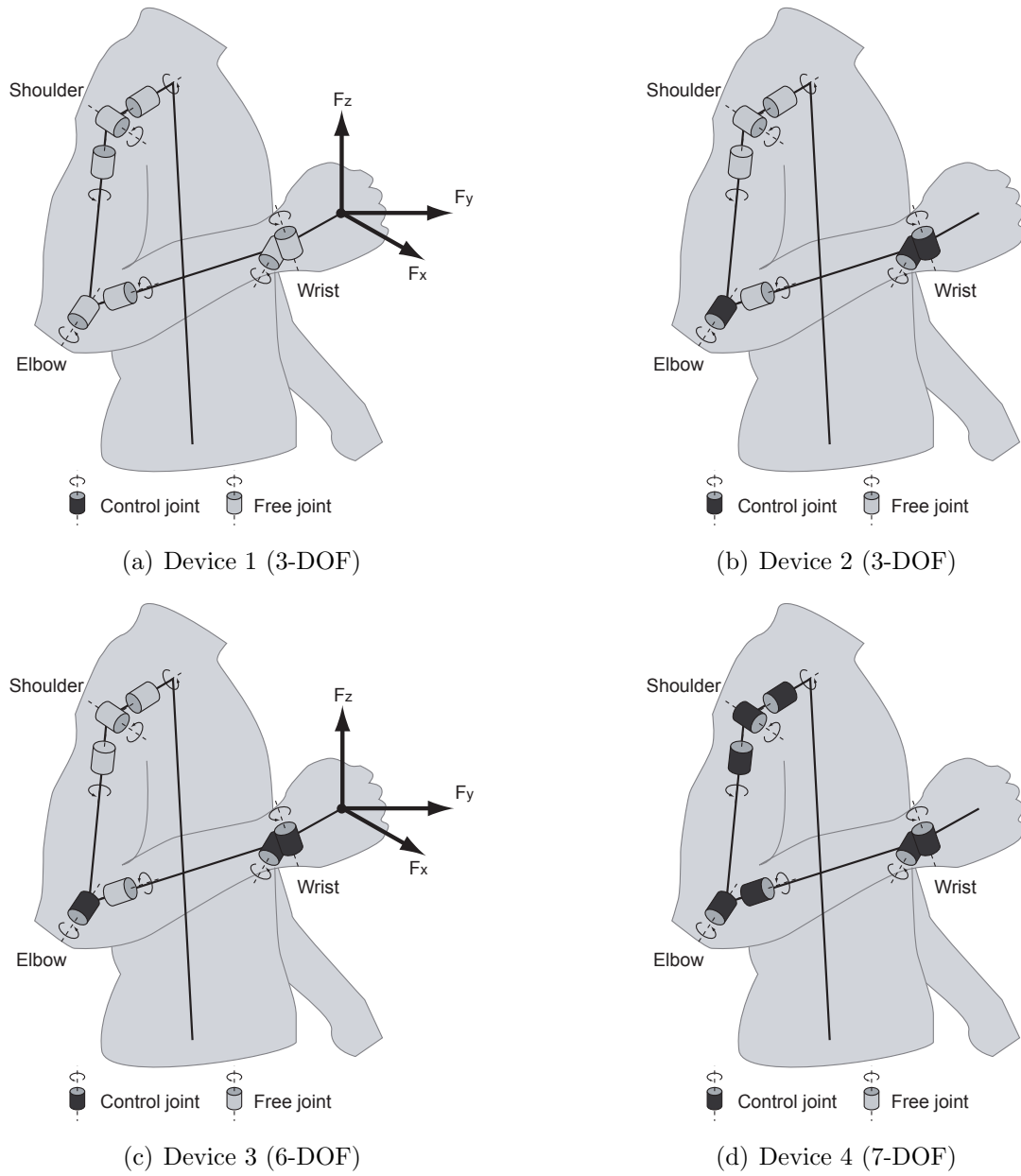
(a) Device 1 (3-DOF)

(b) Device 2 (3-DOF)

(c) Device 3 (6-DOF)

(d) Device 4 (7-DOF)

Figure 5.5. DOF of assisting devices

· Device 1: The device applies 3-DOF forces to hand, e.g. using a robot manipulator.

· Device 2: The device applies 3-DOF joint torques to elbow and wrist joint, e.g. using a power-assisting suit.

· Device 3: The device applies 6-DOF forces (3-DOF forces to hand and 3-DOF joint torques to elbow and wrist joint), just as using Device 1 and 2 simultaneously.

· Device 4: The device applies all 7-DOF joint torques of human arm including wrist, elbow and shoulder joint.

Figure 5.5 shows these device and DOF of control. The Jacobian Matrix of each device was also be checked, and the really controllabe DOF is same as the DOF of control the posture in this simulation ($\theta_{elbow} = 90$[deg]). Black means it is a joint with control and gray means it is free joint. The average value of the change rates for non-target muscle are calculated represent the effect for each device. Hereafter the average value is called as effect rate v, which is defined as:

$$v \triangleq \frac{1}{N} \sum_{j=1}^{N} \left(\frac{\Delta f_j}{f_{0j}} \right) \times 100\%. \tag{5.1}$$

Three target muscles were controlled independently, Flexor Carpi Ulnaris (FCU., No.33), Biceps (BIC., No.25) and Deltoideus (DEL., No.17). The desired force for each muscles are given to 1.5 times of nominal force, $\gamma_j = 1.5$.

Figure 5.6 shows the results of average rate of each device. $v = 0$ means the device cannot realize the desired muscle force of target muscle. Figure 5.6(a) shows that each device can realize the desired muscle force of Flexor Carpi Ulnaris. The effect for non-target muscles was reduced with the increase of control DOF. Figure 5.6(b) and 5.6(c) shows that Device 2 cannot realize the desired muscle force of Biceps and Deltoideus. It is because of that Device 2 can control elbow and wrist joints, but cannot give any force to the muscle of shoulder since one function of these 2 muscles is to move shoulder. For other devices, a similar result was obtained. Especially, all the results of Device 1 (tip force control) show that desired muscle forces of every muscles can be realized. This is because of that the
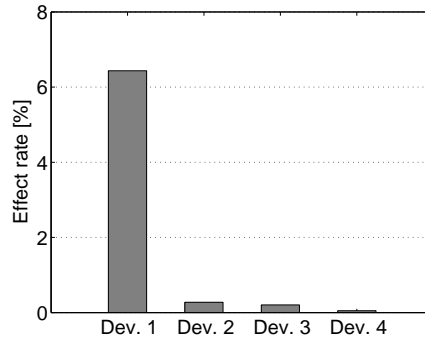
(a) Flexor Carpi Ulnaris (No. 33)×1.5
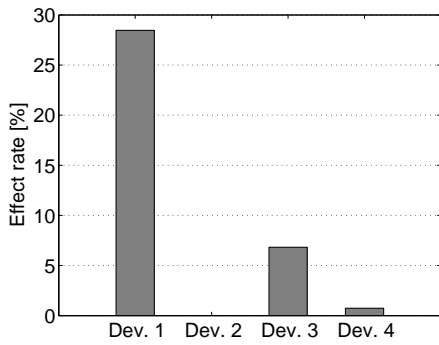
(b) Biceps (No. 25)×1.5
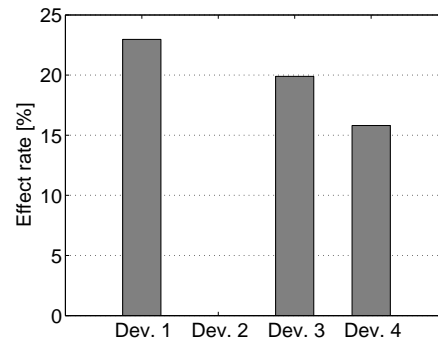
(c) Deltoideus (No. 17)×1.5

Figure 5.6. Effect of the DOF of power-assisting devices

tip force in human hand can change all joint of human manipulator. However, since more than one joint torque were changed simultaneously, the effect rate of non-target muscle is larger than other device.

These results show that, the device with low-DOF also can be used for PMFC using the method proposed in Section 3.3. However, for realizing the desired force, the device need to have the same function with the target muscle.

Chapter 6

Muscle Force Control Experiment

Muscle force control experiments for the same posture used in simulation (Fig. 5.1(a)) are conducted by using the wearable and unwearable robotics device introduced in Section 4.2. Surface electromyography (EMG) signal are measured in each experiments to validate the tendency of muscle force change (e.g. increase or reduce). The measuring and the processing methods of EMG is introduced in Appendix D.

In this chapter, we verify the accuracy of muscle force estimation used in this research at first. Then two power-assisting devices are examined to control the muscle force using the PMFC method. Finally, two power-assisting devices are used simultaneously to check the effect of the different DOF of power-assisting device for PMFC.

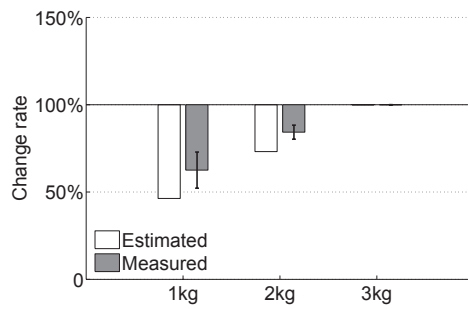## 6.1   Accuracy of muscle force estimation

The validity of the muscle force estimation used in this research (described in Appendix A.3) is confirmed by comparing the change rate of EMG signals and that of the estimated result. In this experiment, 1[kg], 2[kg] and 3[kg] load are applied to the hand of subjects by holding iron dumbbells and the elbow joint is flexed to 90[deg] as used in simulation (Fig. 5.1(a)). The EMG signals of three muscles, Brachialis (BRA), Brachioradials (BRD) and Flexor Carpi Ulnaris (FCU), were measured. The EMG measurement positions for each muscle are shown in Fig. D.1. The data of 3[kg] was considered as the base value, which was used to calculated the change rate of muscle forces in simulation and EMG signals in experiments. The accuracy of muscle force estimation is shown by estimation error, which is defined as the different of these two change rates.

43
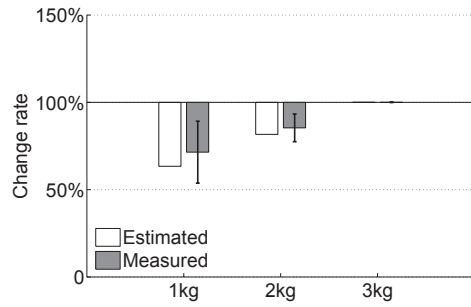
(a) Brachialis
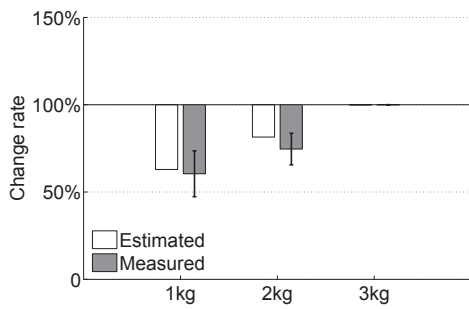
(b) Brachioradials

(c) Flexor carpi ulnaris

Figure 6.1. Results of accuracy verification experiment of muscle force estimation

Table 6.1. Difference of muscle force change
(Difference = |Desired − Measured|)

Muscle	BRA	BRD	FCU	Avg.
1[kg]	8%	2%	16%	9%
2[kg]	4%	7%	11%	7%
3[kg]	-	-	-	-
Avg.	6%	5%	14%	8%

Result

Each experiment was conducted for eight male subjects. Each weight was tested five times for every subject. Ten seconds EMG data was measured in each test and five seconds stable data was used to analyze the change of human muscle force. Figure 6.1 shows the result of change rates. White boxes show the change rates of muscle force estimated from musculoskeletal model; Black boxes show the average change rates of EMG signals measured in experiments. Error lines show the standard deviation (SD) of eight subjects.

As shown in the graphs, same changing tendencies were obtained by comparing the change of EMG signals and estimated value. Table 6.1 shows the difference of change rate between simulation and experiment. The average error for Brachialis was 6%, for Brachioradials is 5%, and for Flexor Carpi Ulnaris was 14%. The average error for all experiments is 8% and the maximum error was 16%. The error between simulation and measurement was small enough. It shows that the musculoskeletal model is valid and can be used in rough muscle force estimation. However, EMG signal are not accurate enough to measure the amount of change since the relation between the magnitude of muscle force and the one of the corresponding EMG signals is not necessarily linear.

6.2 Wearable device

In this experiment, the power-assisting suit introduced in Section 4.2.1 was used for examining the PMFC method. In this experiment, the target muscles are set to Brachialis (No.27), Brachioradials (No.28), and Flexor Carpi Ulnaris (No.33). Eleven sets of desired change rates were given as shown in Table 6.2 for controlling three target muscles independently. For example, Experiment I, J are to support only Flexor Carpi Ulnaris, Experiment C, G are to support only Brachialis and Brachioradials, and other Experiments are the mixture of support and training for these three target muscles. Since Brachialis and Brachioradials are physiologically coupled, these two muscles are treated as a group and given the same change rates. The feasibility for all the five experiments has been confirmed. Table 6.3 shows the target torques of elbow and wrist joints calculated by muscle force control simulation, which are realized by the power-assisting suit

introduced in Section 4.2.1. Table 6.4 shows the driving force of each actuator in power-assisting suit calculated by the device model shown in Fig. 4.3(b). Since a antagonistic construction is used for each joint in power-assisting suit, only 4 actuators have to be controlled in each experiment.

Result

Each experiment was conducted for eight male subjects. Each control was tested five times for every subject. In each control, ten seconds EMG data was measured and five seconds stable data was used to analyze the change of human muscle force. Figure 6.2 shows the results. White and black boxes show the desired and measured changes of the muscle forces.

As shown in the graphs, all the tendencies of the change among the EMGs are as expected. For example, in Experiment A-D, the desired muscle force change rates of Brachialis (BRA) and Brachioradials (BRD) were fixed to 50% and the changes of measured EMG signals for these two muscles were stayed within 67% to 88%; Compared with this, the desired muscle force change rate of Flexor Carpi Ulnaris (FCU) increased from 50% to 125% and the changes of measured EMG signals for this muscle were increased similarly, from 70% to 101%. On the other hand, in Experiment A, E and I, the desired muscle force change rates of Flexor Carpi Ulnaris were fixed to 50% and the changes of measured EMG signals for this muscle were stayed within 67% to 72%; the desired muscle force change rate of other two target muscles are given as 50% and 100% and the changes of measured EMG signals for these two muscles were increased from 71% to 84% and from 69% to 86%.

Table 6.5 shows the control error for each muscle in all experiments. The average control error for all muscle forces were from 11% to 19%; for each experiments were from 2% to 33%; and it for all experiments was about 15%.

These results show the validity of the PMFC method by using the wearable power-assisting device. However, in some experiment (e.g., Experiment C and D), the control errors for some muscles were not so small to obtain good control accuracy due to the weak output power of the device.

Table 6.2. Desired change rate of target muscle force

Experiment	BRA BRD	FCU	BIC
A	×50%	×50%	×101%
B	×50%	×75%	×101%
C	×50%	×100%	×101%
D	×50%	×125%	×101%
E	×75%	×50%	×101%
F	×75%	×75%	×101%
G	×75%	×100%	×101%
H	×75%	×125%	×101%
I	×100%	×50%	×100%
J	×100%	×75%	×100%
K	×100%	×100%	×100%

Table 6.3. Target joint torque

[Nm]

Experiment	τ_{elbow}	$\tau_{wrist1}{}^{*}$	$\tau_{wrist2}{}^{**}$
A	-1.27	-0.15	-0.22
B	-1.15	-0.05	-0.08
C	-1.02	0.05	0.07
D	-0.90	0.16	0.21
E	-0.76	-0.18	-0.26
F	-0.64	-0.08	-0.12
G	-0.51	0.03	0.03
H	-0.39	0.13	0.18
I	-0.25	-0.21	-0.29
J	-0.12	-0.10	-0.14
K	0.00	0.00	0.00

* Dorsal and palmar flexion joint in wrist

** Radial and ulnar flexion joint in wrist

Table 6.4. Output power of artificial muscles

[N]

Experiment	F_1	F_2	F_3	F_4	F_5	F_6	F_7	F_8
A	7.78	7.36	0.00	0.00	0.64	8.61	0.00	0.00
B	7.02	6.64	0.00	0.00	0.35	2.93	0.00	0.00
C	6.26	5.92	0.00	0.00	0.00	0.00	2.65	0.87
D	5.50	5.20	0.00	0.00	0.00	0.00	8.11	3.11
E	4.65	4.40	0.00	0.00	0.62	9.98	0.00	0.00
F	3.89	3.68	0.00	0.00	0.32	4.30	0.00	0.00
G	3.13	2.96	0.00	0.00	0.00	0.00	1.32	0.43
H	2.37	2.24	0.00	0.00	0.00	0.00	6.79	2.68
I	1.52	1.44	0.00	0.00	0.59	11.36	0.00	0.00
J	0.76	0.72	0.00	0.00	0.30	5.68	0.00	0.00
K	0.00	0.00	0.00	0.00	0.00	0.00	0.00	0.00

Table 6.5. Control error in power-assisting suit

(Error = |Desired − Measured|)

Experiment	BRA	BRD	FCU	BIC	Avg.
A	21%	20%	20%	26%	20%
B	32%	17%	0%	13%	16%
C	28%	27%	2%	9%	19%
D	36%	38%	24%	1%	33%
E	6%	1%	22%	14%	10%
F	3%	0%	2%	12%	2%
G	14%	2%	4%	6%	7%
H	23%	1%	17%	12%	14%
I	15%	14%	17%	8%	15%
J	13%	18%	4%	6%	12%
K	-	-	-	-	-
Avg.	19%	14%	11%	11%	15%

(a) Experiment A

(b) Experiment B

(c) Experiment C

(d) Experiment D

(e) Experiment E
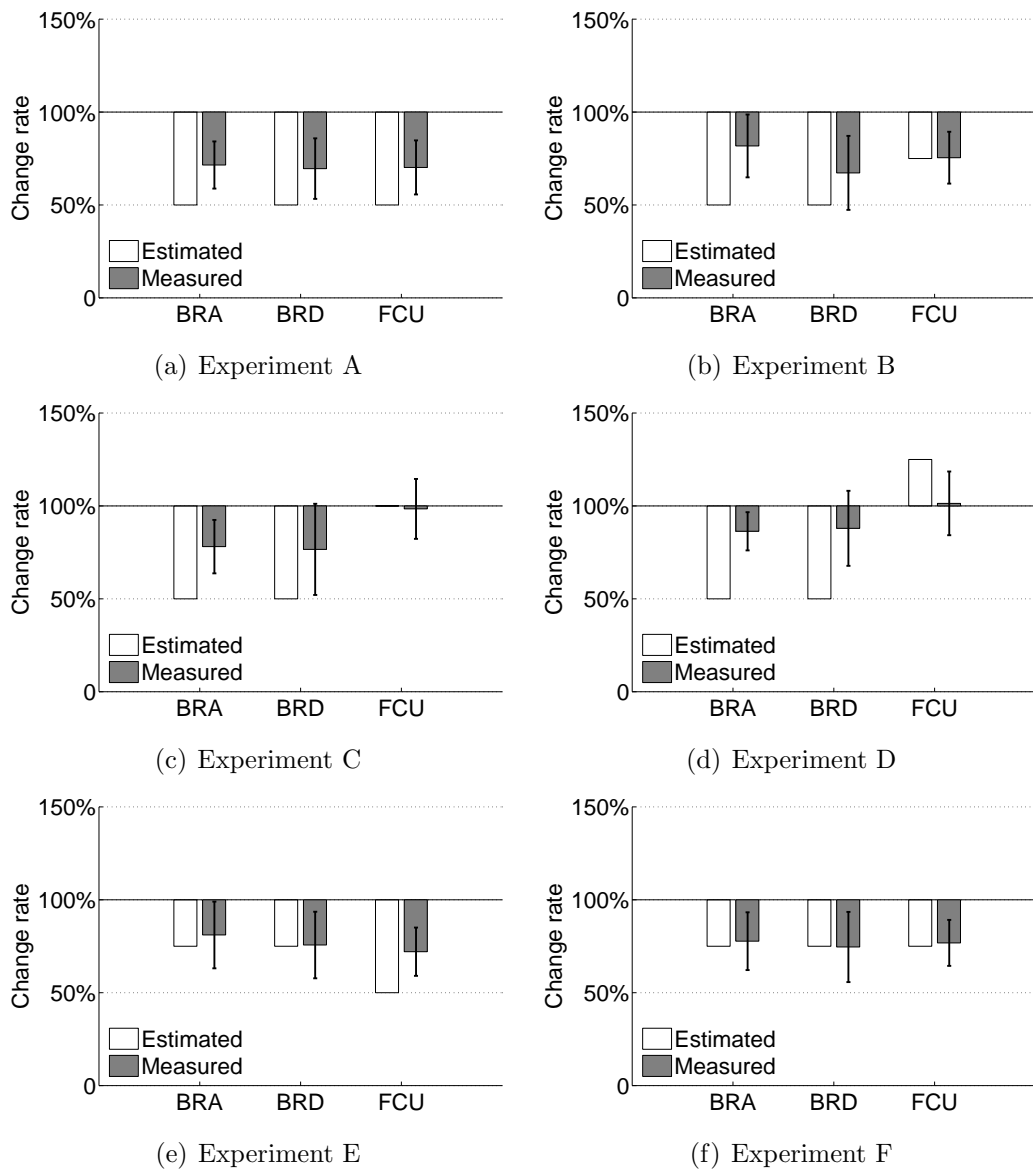
(f) Experiment F

Figure 6.2. Results of muscle force control in power-assisting suit

49

(a) Experiment G

(b) Experiment H

(c) Experiment I

(d) Experiment J

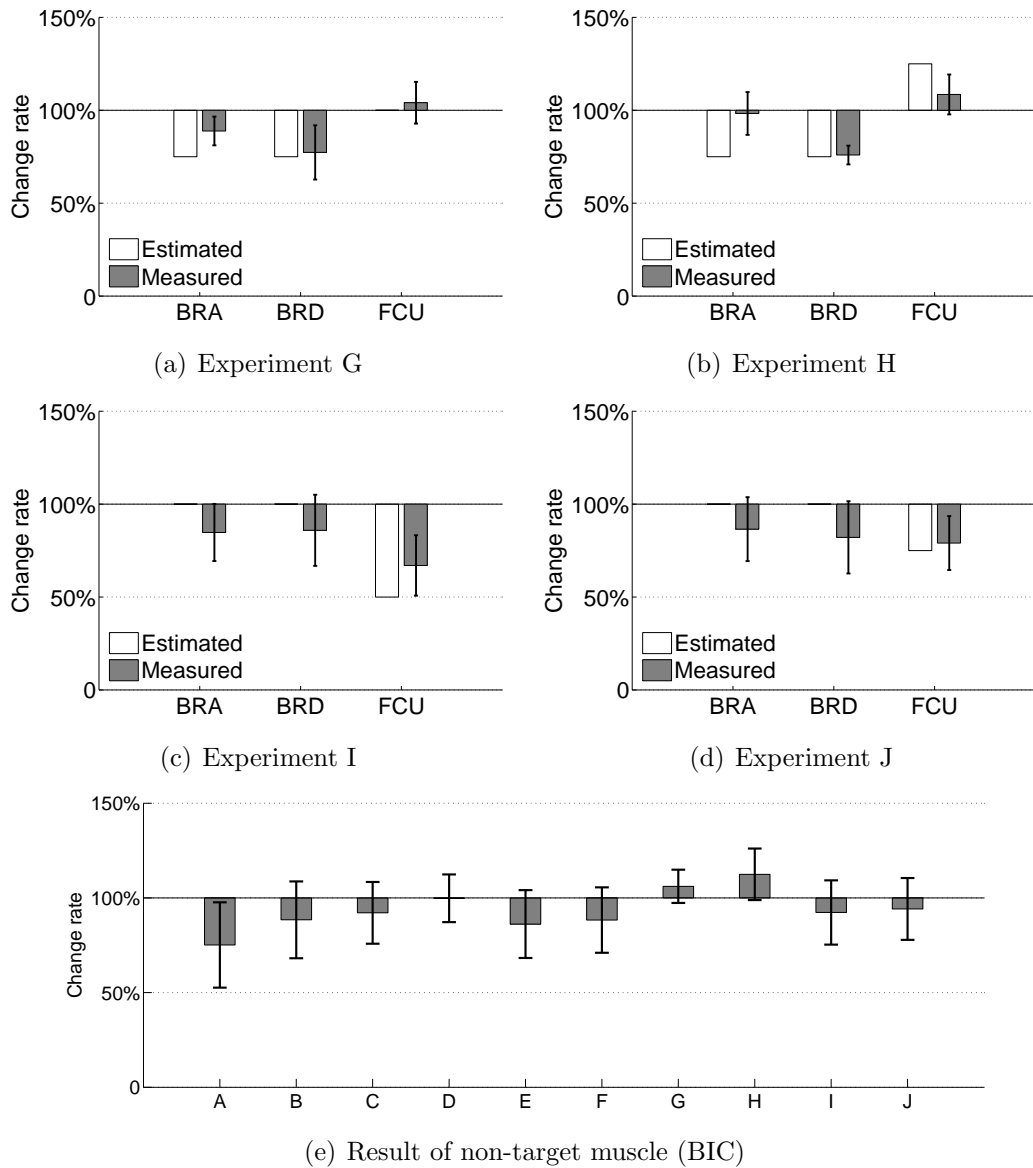(e) Result of non-target muscle (BIC)

Figure 6.3. Results of muscle force control in power-assisting suit (continue)

6.3   Unwearable device

In this experiment, the robot manipulator introduced in Section 4.2.2 was used for examining the validity of PMFC method as an unwearable device. Deltoideus (No.17) and Biceps (No.25) were set as target muscles. The desired change rates of target muscles were given as shown in Table 6.6. Experiment A was considered as the nominal case. In this experiment, a downward force $F_e = 30[\text{N}]$ was applied to the hand. All other change rates of Experiment B - G were based on the value of Experiment A. Experiment B was only to control Deltoideus to 2.0 times. Experiment C was only to control Biceps to 1.5 times. Experiment D gave a mixture control to make both Deltoideus and Biceps to 2.0 and 1.5 times. On the contrary, Experiment E, F and G were controlled to reduce the muscle force individually or together. Experiment E and F were to control Deltoideus and Biceps to 0.5 times of nominal muscle force individually. Experiment G was to control both Deltoideus and Biceps to half of nominal muscle force together. Table 6.7 shows the driving-forces in each experiments calculated in simulation, which are realized by control the robot manipulator. X is front-back direction; Y is left-right direction; Z is up-down direction.

Result

Each experiment was also conducted for eight male subjects. Same as other experiments, in this experiment, each control was also tested five times for every subject. Five seconds stable EMG data in all ten seconds measured data was used to analyze the change of human muscle force. Figure 6.4 shows the results. As shown in previous figure, the white boxes show the desired value and the black boxes show the value calculated from the measured EMG signals.

In Experiment B, the desired muscle force of Deltoideus was given as 200% of nominal muscle force and Biceps was not change after control; EMG signal results also show that the change of Deltoideus was larger than Biceps. In Experiment C, the desired muscle force of Biceps was given as 150% of nominal muscle force and Deltoideus was not change. EMG signal shows the similar results that the change of Biceps was larger than Deltoideus. Simuilarly, in Experiment D, the desired muscle forces of Deltoideus and Biceps were given as 200% and 150%

Table 6.6. Desired change rate of target muscle force

Experiment	Deltoideus (No.17)	Biceps (No.25)
A	$\times 100\%$	$\times 100\%$
B	$\times 200\%$	$\times 100\%$
C	$\times 100\%$	$\times 150\%$
D	$\times 200\%$	$\times 150\%$
E	$\times 50\%$	$\times 100\%$
F	$\times 100\%$	$\times 50\%$
G	$\times 50\%$	$\times 50\%$

Table 6.7. Control force of robot manipulator

Experiment	F_X [N]	F_Y [N]	F_Z [N]
A	0.00	0.00	-30.00
B	-38.87	1.47	-32.99
C	19.87	-0.73	-48.17
D	-18.95	1.70	-51.33
E	19.35	-2.56	-28.18
F	-19.92	-0.30	-11.64
G	-0.54	-2.34	-9.92

Table 6.8. Control error in robot manipulator
(Error = |Desired − Measured|)

Experiment	Deltoideus (No.17)	Biceps (No.25)	Avg.
B	9.5%	28.1%	18.8%
C	43.9%	17.0%	30.4%
D	57.5%	75.1%	66.3%
E	14.0%	12.2%	13.1%
F	10.2%	13.7%	11.9%
G	7.7%	4.5%	6.1%
Avg.	23.8%	25.1%	24.4%

(a) Experiment B

(b) Experiment C

(c) Experiment D

(d) Experiment E
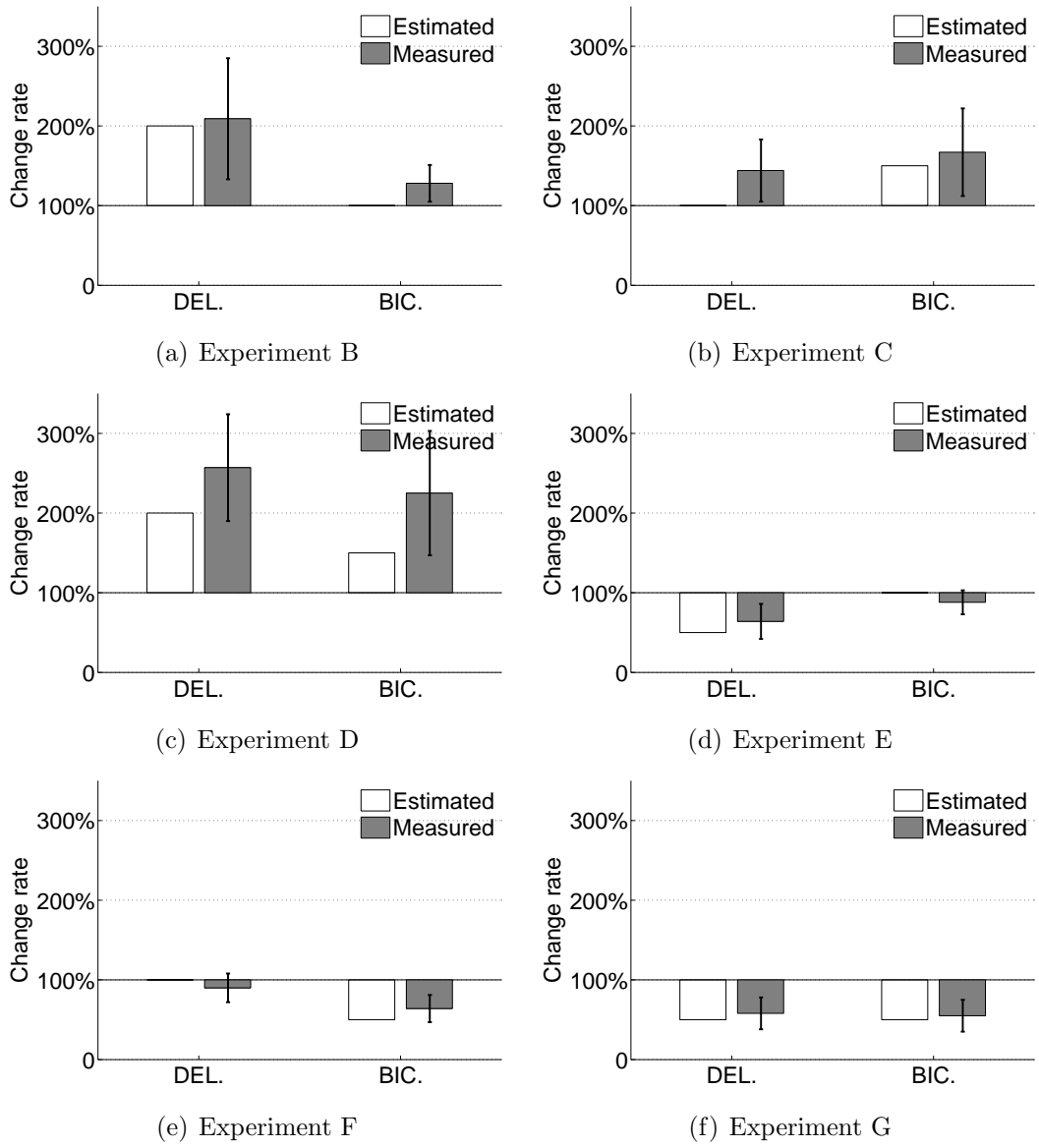
(e) Experiment F

(f) Experiment G

Figure 6.4. Result of muscle force control in robot manipulator

times of nominal muscle force. The results of EMG signal show that two muscle forces were both increased. In the other hand, in Experiment E, F and G, EMG signal results are also shows that all the tendencies are as the desired muscles force.

The control errors of change rate between desired muscle force and the measured EMG signals are shown in Table 6.8. The average control error of Deltoideus and Biceps were 23.8% and 25.1%. The average of all experiments is 24.4%. These results imply that the decrease and increase of target muscle force could been realized not only by simulation but also by experiments. The validity of the PMFC method is also confirmed by using the unwearable power-assisting device.

6.4 Multiple device

In the experiment shown in Fig. 6.5, more than one devices were used to confirm the effect from the DOF of power-assisting device. A power-assisting suit (1-DOF torque-controllable for elbow joint) and a robot manipulator (3-DOF force-controllable of human hand) were used. Biceps (No.25) was set as target muscle. Through the simulated calculation, the desired change rates of this target muscle was fixed to 70%, which can be realized by each device. Same as other experiments, a downward force $F_e = 30[\text{N}]$ was applied to the hand as the nominal case. Two experiments have been conducted by using two devices singly or simultaneously. In Experiments A, target muscle force was only controlled by the robot manipulator. In Experiments B, target muscle force was controlled by both power-assisting suit and robot manipulator simultaneously. In each experiment, other three muscles, Deltoideus (No.17), Brachioradials (No.28) and Flexor Carpi Ulnaris (No.33) were also measured for checking the change of non-target muscle.

Table 6.9 shows the average effect non-target muscle force in each control in simulation. For comparing with experimental results, the effect only for measuring three non-target muscles was also calculated. The DOF of the power-assisting device used in Experiment B is larger than that in Experiment A. Therefore the effect for non-target muscle in Experiment B is smaller than that in Experiment A. Table 6.10 shows the target driving-forces and the joint torque in each experiments calculated in simulation, which are used to control the robot manipulator
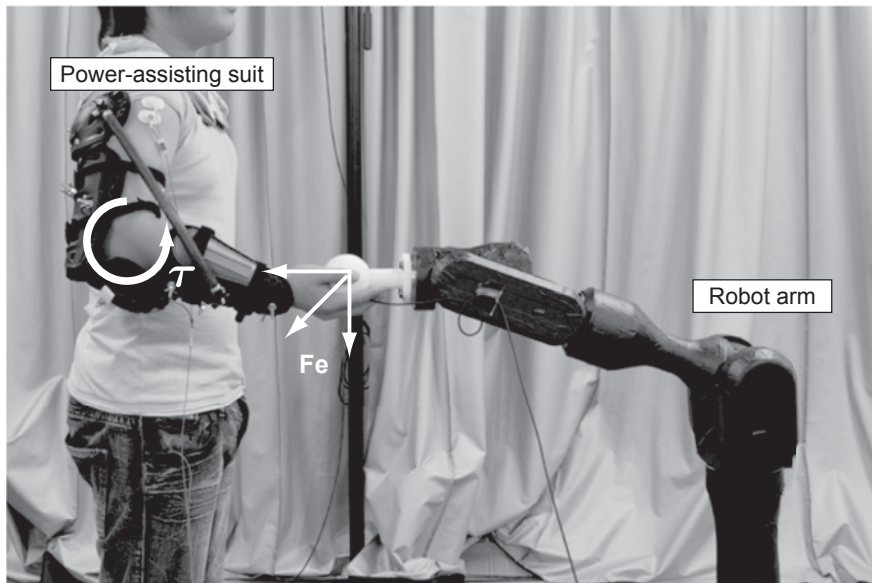
Figure 6.5. Muscle force control using multiple device

and power-assisting suit.

Result

Each experiment was conducted for eight male subjects. Each control was tested five times for every subject. Five seconds stable EMG data in all ten seconds measured data was used to analyze the change of human muscle force. Figure 6.6 shows the results. As shown in other figure, the white boxes show the desired value and the black boxes show the value calculated from the measured EMG signals.

Figure 6.6(a) shows the change rates of target muscle. In both Experiment A and B, the desired muscle force of target muscle was set to 70%. Though the power-assisting device can not control the joint torque perfectly and the control accuracy of Experiment B was lower than Experiment A, the same tendencies was gained and the target muscle - Biceps has been supported in both these two experiments as other single device control experiments. The change rate of target muscle in Experiment A was 78% and that in Experiment B was 85%.

Figure 6.6(b) shows the average effect rate of three measuring non-target

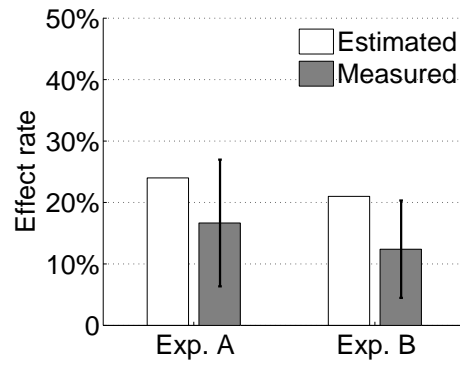Table 6.9. Average effect of non-target muscle in simulation

Experiment	A	B
All non-target muscle	11%	6%
Measured non-target muscle	24%	21%

Table 6.10. Control force and torque

Experiment	F_X [N]	F_Y [N]	F_Z [N]	$\tau_{elbow}[Nm]$
A	-0.41	-18.13	-10.84	-
B	0.92	-25.94	-3.36	0.96
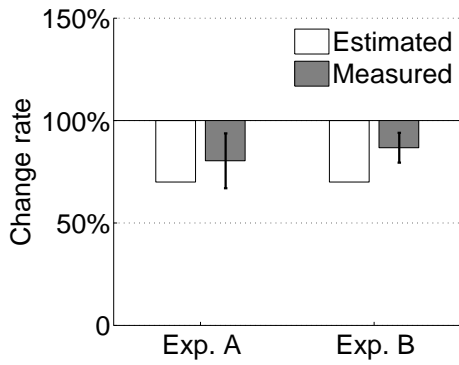
(a) Change rate of target muscle force

(b) Average Effect rate of non-target muscle

Figure 6.6. Result of multiple device control

muscle calculated in (5.1). Same as the result estimated in simulation, the effect of non-target muscle in Experiment A was larger than that in Experiment B. Comparing Experiment B to Experiment A, with the increase of control DOF, the average effect of non-target muscle is reduced from 24% to 21% in simulation. In experiments, it also reduced from 15% to 12%. These results show that, same as shown in simulation, high control DOF device can reduce the effect of non-target muscle.

Chapter 7

Conclusion and Future works

This dissertation proposed a Pinpointed Muscle Force Control (PMFC) method to control the load of selected muscles by using the power-assisting devices, thus enabling pinpointed motion support, rehabilitation, and training by explicitly specifying the target muscles. By taking into account the physical interaction between human muscle forces and actuator driving forces during power-assisting, the feasibility of pinpointed muscle force control is analyzed as a constrained optimization problem. Using the PMFC method, the driving forces of power-assisting devices can be calculated via mathematical analysis of the minimizing problem of muscle force estimation.

In order to designate and control the muscle force easily, a control system, named Muscle Assist System (MAS), was developed. The software of this system is composed of four modules: the posture measurement module, the muscle force estimation module, the muscle force setting module and the device control module. A power-assisting suit and a robot manipulator were used for controlling the muscle force in this research. The driving forces of these robots were controlled in feedback controller to realize the joint torque calculated by software.

In simulation, the feasibility of single and multiple muscle force control were tested. Simulation result showed that single or multiple muscle can be controlled by the pinpointed muscle force control method. Increasing the DOF of power-assisting device may reduce the effect of non-target muscles. The method was also tested in experiments by measuring the surface electromyography (EMG) signals of target and non-target muscles. Similar tendencies of the change were obtained by comparing the change of EMG signals measured in experiments with the estimated change of target muscle force. Most controls are accurate enough and the average control errors are 15% in wearable robotic device and 24.4% in robot manipulator. The effect of non-target muscle from the DOF of power-assisting device was also tested by using multiple devices simultaneously. The result of EMG signal shows that the effect of non-target muscle was decreased

if we increase the DOF of device, which is similar to the result calculated in simulation. These results showed that the PMFC method we proposed is valid.

Future work of this research should mainly focus on the following area:

1. Test the method in more various postures and tasks and test more subjects to confirm the PMFC. At present, due to the limitation in time and device, only a few subject experiments were conducted. In the future, this PMFC method has to be test in more subjects for longer period and for not only static task but also active task.

2. Improve the muscle force design method to increase the control accuracy and reduce the effect of non-target muscle. In the current method, in order to enable to check the feasibility of the desired force of target muscle, inactive muscle has to keep inactive, which limits design of target muscle and increass the effect of non-target muscle. The main task in this area is how to develop a design method to make these inactive muscle force can be changed after control.

3. Develop a more efficient and user-friendly system. Power-assisting device have to be designed more safely and easier to wear and operate. The control software needs to be developed for simplifying target muscle force configuration and designation. A easy to understand result display system is also need to let user check the design and control results.

4. Investigate this method in clinical experiments and test its verification for neurological diagnosis and treatment planning.

Acknowledgements

my difficult moments and their cheerfulness during joyful ones.

Particular thanks go to my parents and family, whose unwavering love and support goes beyond limits and provides me with strength to pursue my studies.

References

[1] Nicholas Yagn, "Apparatus for facilitating walking, running and jumping," US Patent No. 420179, 1890.

[2] Bruce R. Fick and John B. Makinson, "Hardiman I prototype for machine augmentation of human strength and endurance: Final report," General Electric Company Technology Report S-71-1056, 1971.

[3] Homayoon Kazerooni, "Extender: A case study for human-robot interaction via transfer of power and information signals," *IEEE International Workshop on Robot and Human Communication*, pp. 10–20, 1993.

[4] Homayoon Kazerooni, Ryan Steger, and Lihua Huang, "Hybrid control of the berkeley lower extremity exoskeleton (bleex)," *the International Journal of Robotics Research*, vol. 25, no. 5, pp. 561–573, 2006.

[5] Erico Guizzo and Harry Goldstein, "The rise of the body bots," *IEEE Spectrum*, vol. 42, no. 10, pp. 50–66, October 2005.

[6] Ryan Farris, Hugo Quintero, Thomas Withrow, and Michael Goldfarb, "Design and simulation of a joint-coupled orthosis for regulating fes-aided gait," in *2009 IEEE International Conference on Robotics and Automation (ICRA2009)*, Kobe International Conference Center, Kobe, Japan, May 12-17 2009, pp. 1916–1922.

[7] Suwoong Lee and Yoshikuyi Sankai, "Power assist control for walking aid with hal-3 based on emg and impedance adjustment around knee joint," *IEEE/RSJ International Conference Intelligent Robots and Systems*, pp. 1499–1504, 2002.

[8] Keijiro Yamamoto, Kazuhito Hyodo, Mineo Ishii, and Takashi Matsuo, "Development of power assisting suit for assisting nurse labor," *JSME international journal (Series C)*, vol. 45, no. 3, pp. 703–711, 2002.

[9] Daisuke Sasaki, Toshiro Noritsugu, and Masahiro Takaiwa, "Development of pneumatic power assist splint assist operated by human intention," *Journal of Robotics and Mechatronics*, vol. 17, no. 5, pp. 568–574, 2005.

[10] Toshiro Noritsugu, Daisuke Sasaki, Masafumi Kameda, Atsushi Fukunaga, and Masahiro Takaiwa, "Wearable power assist device for standing up motion using pneumatic rubber artificial muscles," *Journal of Robotics and Mechatronics*, vol. 19, no. 6, pp. 617–628, 2007.

[11] Toshiro Noritsugu, Masahiro Takaiwa, and Daisuke Sasaki, "Development of power assist wear using pneumatic rubber artificial muscles," *Journal of Robotics and Mechatronics*, vol. 21, no. 5, pp. 607–613, 2009.

[12] Katsuya Knaoka, "A study on man-machine synergy effect in non-programmable heavy physical work," in *the 11th Symposium on Construction Robotics in Japan (11th SCR)*, September 2008, pp. 119–124.

[13] HONDA Motor Co., Inc., "http://corporate.honda.com/innovation/walk-assist/."

[14] Activelink Co., Ltd., "http://psuf.panasonic.co.jp/alc/en/index.html."

[15] Hermano Igo Krebs, James Celestino, Dustin Williams, Mark Ferraro4, Bruce Volpe, and Neville Hogan, "A wrist extension for mit-manus," *Advances in Rehabilitation Robotics*, pp. 377–390, 2004.

[16] Ying Jin, Takehito Kikuchi, Kazuki Fukushima, Hiroki Akai, and Junji Furusho, "Quasi-3 dof active-passive hybrid rehabilitation system for upper limbs "Hybrid-PLEMO"," *Journal of Japan Society of Mechanical Engineer (C)*, vol. 74, no. 745, pp. 2099–2106, 2008.

[17] Andras Toth, Gusztav Arz, Gabor Fazekas, Daniel Bratanov, and Nikolay Zlatov, "Post stroke shoulder-elbow physiotherapy with industrial robots," *Advances in Rehabilitation Robotics*, pp. 391–411, 2004.

[18] YASKAWA ELECTRIC, "http://www.yaskawa.co.jp/newsrelease/2007/20.htm."

[19] Tomoya Tamei, Shin Ishii, and Tomohiro Shibata, "Virtual force/tactile sensors for interactive machines using the user's biological signals," *Advanced Robotics*, vol. 22, pp. 893–911, November 2008.

[20] Hiroshi Kobayashi, Takamitsu Aida, and Takuya Hashimoto, "Muscle suit development and factory application," *International Journal of Automation Technology*, vol. 3, no. 6, 2009.

[21] MusculoGraphics Inc., "http://www.musculographics.com."

[22] CYBERNET SYSTEMS CO., LTD., "http://www.cybernet.co.jp/anybody/."

[23] Life Modeler Inc., "http://www.lifemodeler.com."

[24] GSport Inc., "http://www.gsport.co.jp/p_l_armo.html."

[25] Taku Komura, Yoshihisa Shinagawa, and Tosiyasu L. Kunii, "Calculation and visualization of the dynamic ability of the human body," *Journal of Visualization and Computer Animation*, vol. 10, no. 2, pp. 57–78, 1999.

[26] Richard L. Lieber, "Skeletal muscle is a biological example of a linear electroactive actuator," in *SPIE's 6th Annual International Symposium on Smart Structures and Materials*, San Diego, CA, USA, March 1-5, 1999.

[27] Roy D. Crowninshield and Richard A. Brand, "A physiologically based criterion of muscle force prediction in locomotion," *Journal of Biomechanics*, vol. 14, pp. 793–801, 1981.

[28] Katayama Masazumi and Kawato Mitsuo, "Virtual trajectory and stiffness ellipse during multijoint arm movement predicted by neural inverse models," *Biological Cybernetics*, vol. 69, no. 5, pp. 353–362, 1993.

[29] Jun Ueda, Masayuki Matsugashita, Reshi Oya, and Tsukasa Ogasawara, "Control of muscle force during exercise using a musculoskeletal-exoskeletal integrated human model," in *10th International Symposium on Experimental Robotics(ISER2006)*, Rio de Janeiro, Brazil, July 6-10 2006.

[30] Dan Karlsson and Bo Peterson, "Towards a model for force predictions in the human shoulder," *Journal of Biomechanics*, vol. 25, pp. 189–199, 1991.

[31] MotCo project, "http://motco.info/data/pcsa.html."

[32] Dimitri P. Bertsekas, *Nonlinear Programming*. 2nd edition, Athena Scientific, 1999.

[33] B. M. van Bolhuis and C. C. A. M. Gielen, "A comparison of models explaining muscle activation patterns for isometric contractions," *Biological Cybernetics*, vol. 81, no. 3, pp. 249–261, September 1999.

[34] Thomas S. Buchanan and David A. Shreeve, "An evaluation of optimization techniques for the prediction of muscle activation patterns during isometric tasks," *Journal of biomechanical engineering*, vol. 118, no. 4, pp. 565–574, 1996.

[35] Kizuka Tomohiro, Masuda Tadashi, Kiryu Tohru, and Sadoyama Tsugutake, *Biomechanism Library - Practical Usage of Surface Electromyogram*. Tokyo Denki University Press, 2006.

[36] Shrawan Kumar, Ed., *Biomechnics in Ergonomics*, Taylor & Francis, ch. 11, p. 212, 1999.

Appendix

A. Musculoskeletal Model

This section describes the musculoskeletal model which was used for the muscle force estimation. Musculoskeletal model is composed of skeleton model and muscle model. In this research, Oya's model[29] is used. This model can be used to estimate the muscle force for static tasks or quasi-static motions of right upper body.

A.1 Skeleton model

Skeleton model is used to obtain the position and direction of human bones in kinematics. The structure of human bones is very complex. Bones are connected to each other by joints. In many cases, the axis of joint is not fixed and changed with rotation. Many research methods are studied for how to measure or estimate the joint axis correctly. However, for uncomplicated movement, simplified model can also get enough accuracy in low calculation cost.

In this research, a simplified skeleton model of the human upper-right limb shown as Fig. A.1(a) was developed to calculate the position of each link and the torque of each joint. This model consists of 5 rigid links with 12 joints corresponding to the waist, neck, shoulder, elbow, and wrist. Figure A.1(b) shows the coordination of each joint which is used for kinematic calculation.

A.2 Muscle model

Muscle is the contractile tissue of human, which is classified as skeletal, cardiac, or smooth muscle. In musculoskeletal model, only skeletal muscle is considered because only this type of muscle is anchored to bone and is used for effect skeletal movement such as locomotion and in maintaining posture.

In this research, 41 muscles of the upper right limb are modeled as massless wire. All muscles are anchored to bones from start point to through point and end point. In order to estimate the muscle force accurately and easily, branched
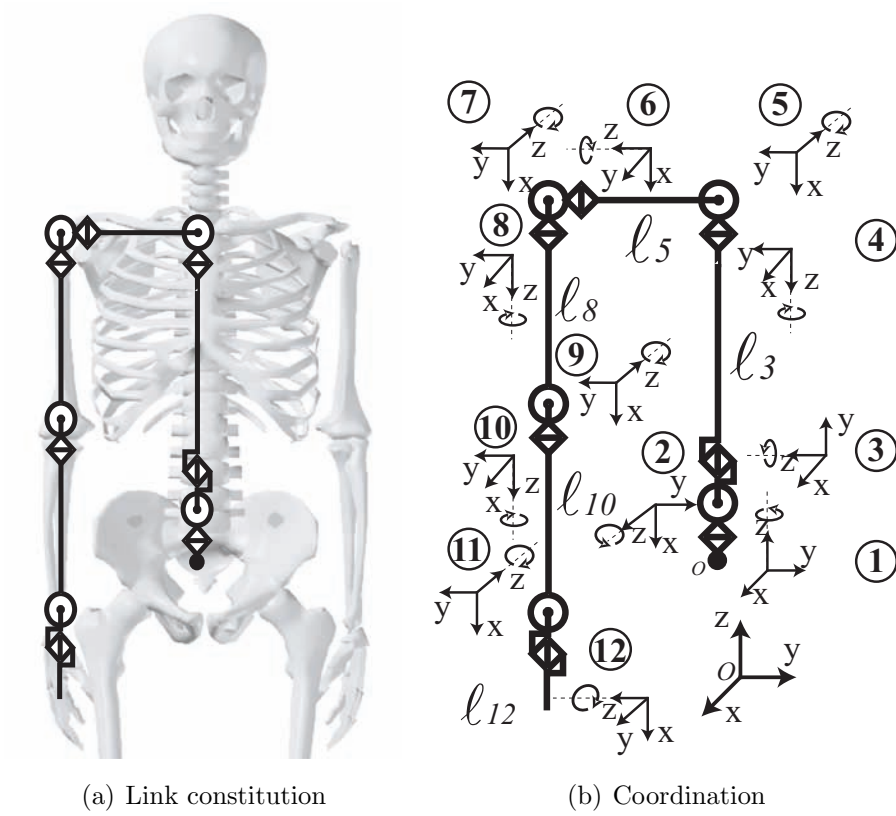
(a) Link constitution   (b) Coordination
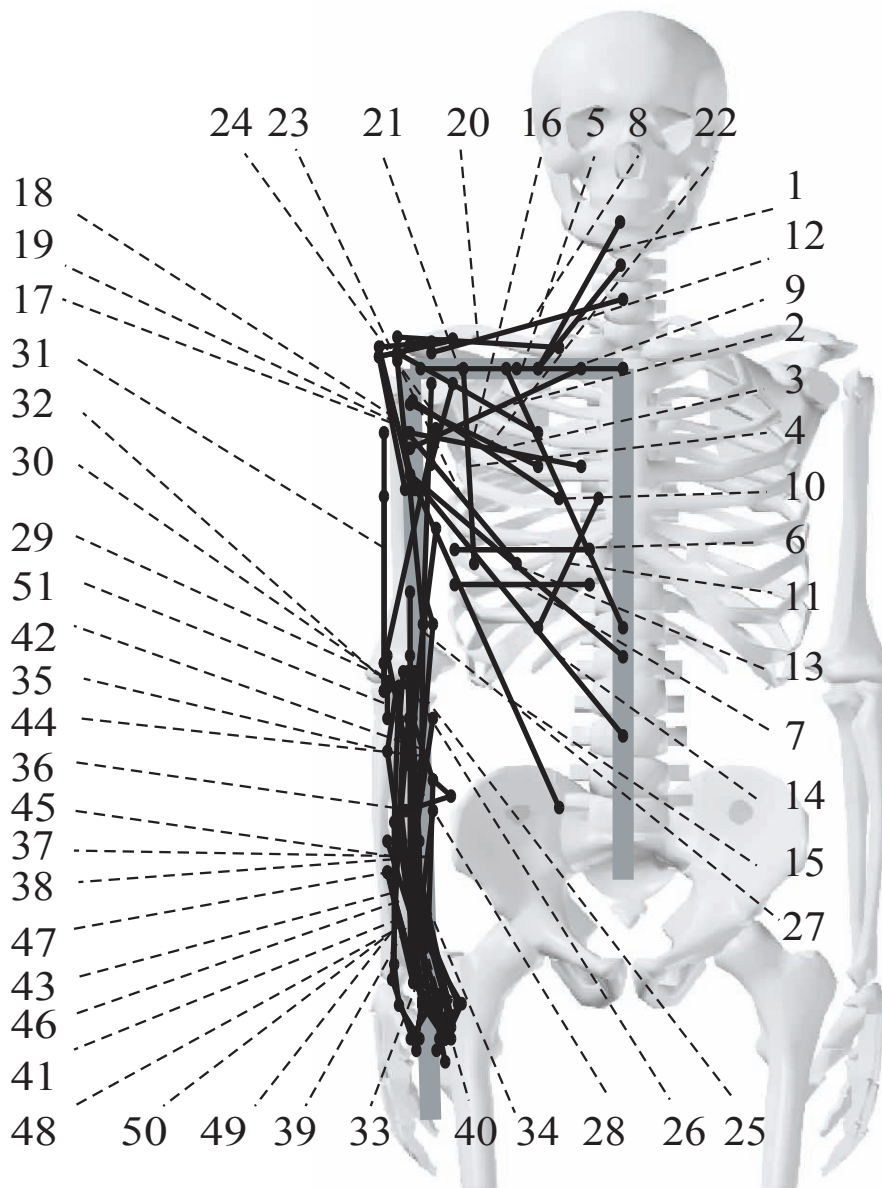
Figure A.1. Skeleton model of the right upper body

Figure A.2. Muscle model of the right upper body

muscle (e.g. Biceps, Deltoideus, etc.) and large muscle (e.g. Trapezius, Latissimus dorsi, etc.) are separated to two or three muscles. Eventually, 41 muscles are modeled as 51 wires shown as Fig. A.2. Table A.1 lists the names and the PCSA of all model we modeled.

A.3   Muscle force estimation method

Suppose that the human musculoskeletal model has M joints and N muscles. Let $\boldsymbol{f} = [f_1, f_2, \cdots, f_N]^T$ be a contraction force vector of human muscles. The relation between the human joint torque $\boldsymbol{\tau}_h \in \boldsymbol{R}^M$ and $\boldsymbol{f}$ are given by

$$\boldsymbol{\tau}_h = \boldsymbol{A}\boldsymbol{f} = \begin{bmatrix} a_{11} & \cdots & a_{1N} \\ \vdots & \ddots & \vdots \\ a_{M1} & \cdots & a_{MN} \end{bmatrix} \begin{bmatrix} f_1 \\ \vdots \\ f_N \end{bmatrix}, \tag{A.1}$$

where $\boldsymbol{A}$ is a moment arm matrix of the muscles. The element a_{ij} denotes the moment arm of muscle j for joint i. $a_{ij} = 0$ is given if f_j does not affect on joint i. Note that $\boldsymbol{A}$ is a function of joint angles and provided by the musculoskeletal model in the previous section.

Generally human body has a redundant number of muscles than the number of joints, i.e. $N \gg M$, which makes the estimation of muscle forces $\boldsymbol{f}$ from joint torques $\boldsymbol{\tau}_h$ an ill-posed problem. Various optimization approaches have been proposed to model the principle of optimality [27, 33, 34] and to solve this problem by minimizing a cost function. In this research, Crowninshield's cost function [27] is used to solve this problem by minimizing a physiologically based criterion $u(\boldsymbol{f})$ as follows:

$$u(\boldsymbol{f}) = \sum_{j=1}^{N} \left(\frac{f_j}{S_j} \right)^r \rightarrow \min, \tag{A.2}$$

$$\text{such that:} \begin{cases} \boldsymbol{\tau}_h = \boldsymbol{A}\boldsymbol{f}; \\ f_{\min j} \leq f_j \leq f_{\max j \; (j=1,\cdots,N)}, \end{cases}$$

where S_j is the physiological cross sectional area (PCSA), and $f_{\max j} = \varepsilon \cdot S_j$ is the maximum muscle force for muscle j. $\varepsilon = 0.7 \times 10^6 [\text{N/m}^2]$ was given by Karlsson [30] and S_j are found in [31] shown in Table A.1. $\forall j, f_{\min j} = 0$ is used.

Table A.1. List of Muscles in Musculoskeletal Model

No.	Muscle Name	PCSA [mm^2]
1.	Levator Scapulae	283
2.	Pectoralis major Pars clav.	452
3.	Pectoralis major Pars ster.	407
4.	Pectoralis minor	487
5.	Subclavius	200
6.	Serratus anterior superior	700
7.	Serratus anterior inferior	700
8.	Trapezius superiof	530
9.	Trapezius mediums	530
10.	Trapezius inferior	530
11.	Rhomboids major	314
12.	Rhomboids minor	314
13.	Latissimus dorsi superior	283
14.	Latissimus dorsi mediums	283
15.	Latissimus dorsi inferior	283
16.	Subscapularis	1351
17.	Deltoideus Pars clavicularis	863
18.	Deltoideus Pars acromialis	863
19.	Deltoideus Pars spinalis	863
20.	Supraspinatus	521
21.	Infraspinatus	951
22.	Teres major	1020
23.	Teres minor	292
24.	Coracobrachial	251
25.	Biceps brachii Caput longum	321
26.	Biceps brachii Caput breve	308
27.	Brachialis	840
28.	Brachioradials	470
29.	Triceps Caput longum	230

Table A.2. List of Muscles in Musculoskeletal Model (Continue)

No.	Muscle Name	PCSA [mm^2]
30.	Triceps Caput mediale	230
31.	Triceps Caput laterale	230
32.	Anconeus	250
33.	Flexor carpi ulnaris	626
34.	Flexor carpi radialis	360
35.	Palmaris longus	76
36.	Flexor digitorum superficialis 1	309
37.	Flexor digitorum superficialis 2	309
38.	Flexor digitorum profundus	790
39.	Flexor pollicis longus	336
40.	Pronator quadratus	263
41.	Abductor pollicis longus	263
42.	Pronator teres	337
43.	Extensor carpi ulnaris	200
44.	Extensor carpi radialis longus	287
45.	Extensor carpi radialis brevis	396
46.	Digital extensor	485
47.	Extensor digiti Minimi	181
48.	Extensor indicis	178
49.	Extensor pollicis longus	146
50.	Extensor pollicis brevis	134
51.	Supinator	470

B. Karush-Kuhn-Tucker Conditions

This section describes the Karush-Kuhn-Tucker conditions (KKT conditions) used in the muscle force design. KKT conditions are necessary conditions for general equality-inequality constrained problem which was published by Karush, Kuhn and Tucker at 60 years ago.

At first, let us consider the following nonlinear optimization problem.

$$f(\boldsymbol{x}) \to \min, \tag{B.1}$$

$$\text{such that}: \begin{cases} g_i(\boldsymbol{x}) \leq 0 & (i = 1, \cdots, m); \\ h_j(\boldsymbol{x}) = 0 & (j = 1, \cdots, l). \end{cases}$$

where $f(\boldsymbol{x})$ is the objective function to be minimized, $\boldsymbol{x} \in \boldsymbol{R}^n$ is the variable vector with n elements. $g_i(\boldsymbol{x})$ are the inequality constraints and $h_j(\boldsymbol{x})$ are the equality constraints. m and l are the number of inequality and equality constraints.

Suppose that $f(\boldsymbol{x})$, $g_i(\boldsymbol{x})$ and $h_j(\boldsymbol{x})$ are differentiable at a point $\bar{\boldsymbol{x}}$. If $\bar{\boldsymbol{x}}$ is a minimum (or local minimum) which satisfies some regularity conditions, such $\boldsymbol{\lambda} \in \boldsymbol{R}^m$ and $\boldsymbol{\mu} \in \boldsymbol{R}^l$ are exist as following:

$$\nabla_x L(\boldsymbol{x}, \bar{\boldsymbol{\lambda}}, \bar{\boldsymbol{\mu}}) = \nabla_x f(\bar{\boldsymbol{x}}) + \sum_{i=1}^{m} \bar{\lambda}_i \nabla g_i(\bar{\boldsymbol{x}}) + \sum_{j=1}^{l} \bar{\mu}_j \nabla h_j(\bar{\boldsymbol{x}}) = 0; \tag{B.2}$$

$$g_i(\bar{\boldsymbol{x}}) \leq 0, \bar{\lambda}_i \geq 0, \bar{\lambda}_i g_i(\bar{\boldsymbol{x}}) = 0 \quad (i = 1, \cdots, m)); \tag{B.3}$$

$$h_j(\bar{\boldsymbol{x}}) = 0 \quad (j = 1, \cdots, l)). \tag{B.4}$$

C. Optimization Problems

This section describes some special optimization problems and the solution methods used in muscle force estimation and designation.

C.1 Quadratic Programming Problem

Quadratic programming (QP) problem is a special type of mathematical optimization problem which optimizes (minimize or maximize) a quadratic function of several variables subject to linear constraints on these variables.

Quadratic programming problem is formulated as:

$$f(\boldsymbol{x}) = \frac{1}{2}\boldsymbol{x}^T\boldsymbol{Q}\boldsymbol{x} + \boldsymbol{c}^T\boldsymbol{x} \to \min, \qquad (\text{C.1})$$

$$\text{such that} : \begin{cases} \boldsymbol{Ax} \leq \boldsymbol{b}; \\ \boldsymbol{Ex} = \boldsymbol{d}. \end{cases}$$

where $f(\boldsymbol{x})$ is the objective function to be minimized, $\boldsymbol{x} \in \boldsymbol{R}^{n \times 1}$ is the variable vector with n elements. $\boldsymbol{Q}$ is a $n \times n$ matrix, $\boldsymbol{c}$ is a $n \times 1$ vector. If the number of inequality and equality constraints are m and l, $\boldsymbol{A}$ and $\boldsymbol{E}$ are $m \times n$ and $l \times n$ matrixes, $\boldsymbol{b}$ and $\boldsymbol{d}$ are $m \times 1$ and $l \times 1$ vectors.

From optimization theory introduced in Appendix B, a necessary condition for a point $\boldsymbol{x}$ to be a global minimum is to satisfy the Karush—Kuhn—Tucker conditions. Using the KKT condition, we can find the dual of QP problem is also a QP problem. Using Sequential Quadratic Programming (SQP) algorithm, QP problem can be solved.

C.2 Constrained Linear Least-Squares Problem

Linear Least-Squares (LLS) is a computational approach to fitting a mathematical model to data. It can be applied when the idealized value provided by the model for each data point is expressed linearly in terms of the unknown parameters of the model.

Constrained Linear Least-Squares (CLLS) is different from general Linear Least-Squares problem. It is constrained by some inequality and equality constraints.

Quadratic programming problem is formulated as:

$$f(\boldsymbol{x}) = \|\boldsymbol{Cx} - \boldsymbol{d}\|^2 \to \min, \tag{C.2}$$

$$\text{such that :} \begin{cases} \boldsymbol{Ax} \leq \boldsymbol{b}; \\ \boldsymbol{Ex} = \boldsymbol{d}. \end{cases}$$

where $f(\boldsymbol{x})$ is the objective function to be minimized, $\boldsymbol{x} \in \boldsymbol{R}^{n \times 1}$ is the variable vector with n elements. $\boldsymbol{C}$ is a $k \times n$ matrix, $\boldsymbol{c}$ is a $k \times 1$ vector (where k is the sample number). If the number of inequality and equality constraints are m and l, $\boldsymbol{A}$ and $\boldsymbol{E}$ are $m \times n$ and $l \times n$ matrixes, $\boldsymbol{b}$ and $\boldsymbol{d}$ are $m \times 1$ and $l \times 1$ vectors.

(C.2) can be rewritten as followed:

$$\begin{aligned} f(\boldsymbol{x}) &= \|\boldsymbol{Cx} - \boldsymbol{d}\|^2 \\ &= (\boldsymbol{Cx} - \boldsymbol{d})^T(\boldsymbol{Cx} - \boldsymbol{d}) \\ &= \{(\boldsymbol{Cx})^T - \boldsymbol{d}^T\}(\boldsymbol{Cx} - \boldsymbol{d}) \\ &= (\boldsymbol{Cx})^T\boldsymbol{Cx} + \boldsymbol{d}^T\boldsymbol{Cx} + (\boldsymbol{Cx})^T\boldsymbol{d} + \boldsymbol{d}^T\boldsymbol{d} \\ &= \boldsymbol{x}^T\boldsymbol{C}^T\boldsymbol{Cx} + \boldsymbol{d}^T\boldsymbol{Cx} + (\boldsymbol{d}^T\boldsymbol{Cx})^T + \boldsymbol{d}^T\boldsymbol{d} \\ &= \boldsymbol{x}^T\{\boldsymbol{C}^T\boldsymbol{C}\}\boldsymbol{x} + 2\boldsymbol{d}^T\boldsymbol{Cx} + \boldsymbol{d}^T\boldsymbol{d}. \end{aligned} \tag{C.3}$$

Since $\boldsymbol{d}^T\boldsymbol{d}$ is a constant, just minimize the first two terms, $f(\boldsymbol{x})$ can be minimized.

$$f(\boldsymbol{x}) \to \min \iff g(\boldsymbol{x}) = \boldsymbol{x}^T\{\boldsymbol{C}^T\boldsymbol{C}\}\boldsymbol{x} + 2\boldsymbol{d}^T\boldsymbol{Cx} \to \min. \tag{C.4}$$

This new optimization problem $g(\boldsymbol{x})$ is a QP program introduced in Section C.1, where $\boldsymbol{Q} = \boldsymbol{C}^T\boldsymbol{C}$ and $\boldsymbol{c}^T = 2\boldsymbol{d}^T\boldsymbol{C}$.

D. Electromyography (EMG)

This section describes the electromyography (EMG) signal and the proceeding method used in the evaluation experiments. Electromyography (EMG) is a technique to record and express the activation signals of muscles. This activation signals of muscles are also called Myo-Electric Potential (ME potential), which is generated by muscle cells when these cells are both mechanically active and at rest. Two kinds of electrode is wildly used to measure the EMG signal. One is needle electrode, which is stung into the muscle. The measured signal is called as needle EMG signal. This method is invasive for human body however it has high resolution, which is mainly used in clinical discipline, such as neuromuscular disease. The other is surface electrode, which is pasted on the skin surface. The measured signal is called as surface EMG signal. This method is noninvasive for human body. It is not only used in basic research and clinical discipline, but also wildly used many research areas such as sport, rehabilitation, body engineer, and virtual reality (VR) [35].

D.1   EMG signal measurement

Before measuring the surface EMG signal, electrodes need to be pasted on the skin surface. Following steps show the main processing in the arrangement of electrodes.

· At first, find the motor point of the muscle. Motor point is the point at which the motor nerve enters the muscle. Motor points are often located over the center of the belly of the muscle, where the muscle contraction is maximum.

· Second, make sure the direction of the muscle fiber. It can be found from anatomical drawing of the muscle. However, in many cases, it is also necessary to feel the muscle with hand directly to find the moving direction of the belly of the muscle.

· Then, reduce the resistance of skin. Generally, it is sufficient to clean the measurement area with alcohol absorbent cotton. in some cases, for getting

high Signal to Noise ratio (S/N ratio), we should also rub skin on the motor point by cotton swab to remove the cuticle.

· Next, fix the electrodes on the motor point. Two electrodes need to be pasted with the direction of the muscle fiber.

· Finally, paste the grounded electrodes. It has to be paste on the skin under which there is not muscle, e.g. wrist, ankle, cubical, kneecap, etc. The pasted skin also need to be process to reduce the resistance.

In the past, for recoding the EMG signal oscilloscope (OSC) and pen recorder were used. Recently, PC and AD converters are used. Many analysis softwares can be used directly to measure and process the EMG signal. It is best that The sampling frequency of AD converter is larger than 2kHz; at least, 1 [kHz] is necessary. Figure D.1 shows several measurement positions used in this research.

D.2　EMG signal processing

Measured raw EMG signal is shown as Fig. D.2(a). It can be used for qualitative analysis. For quantitative analysis, the following process is well-used for the EMG signal.

· **Detrend:** Remove DC offset from the raw EMG signal. (Fig. D.2(b))

· **Rectification:** Translates the Detrended EMG signal to a single polarity (usually positive). (Fig. D.2(c))

· **Low-pass:** Smooth the Rectified EMG signal. (Fig. D.2(d))

· **Integration:** Calculate integration value of the EMG signal (Rectified or filtered EMG signal), which is called as IEMG. For example, the IEMG of the signal shown in Fig. D.2 is about 0.016. In this research, IEMG data is used to reflect the largeness of muscle force for a specified period.
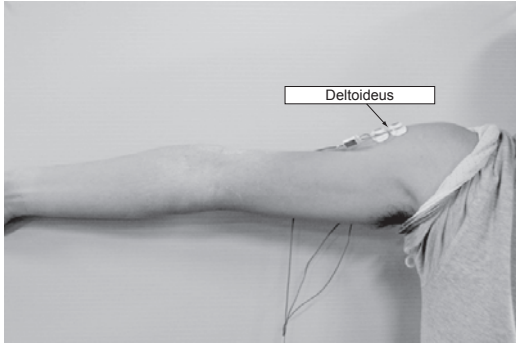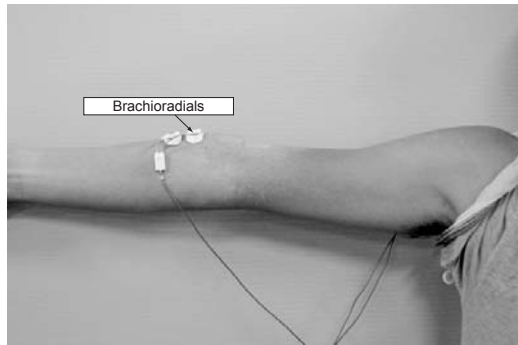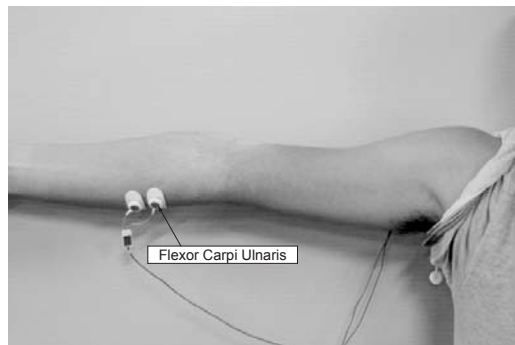
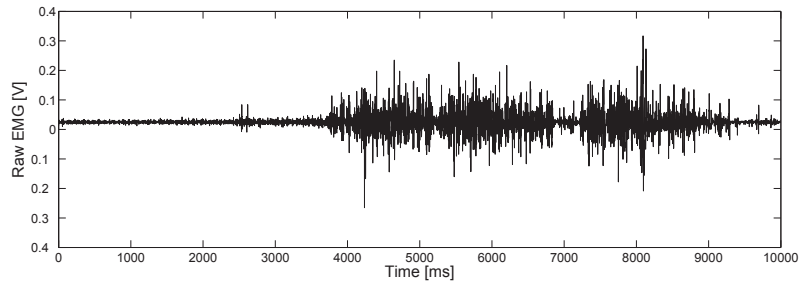(a) Deltoideus (No.17)
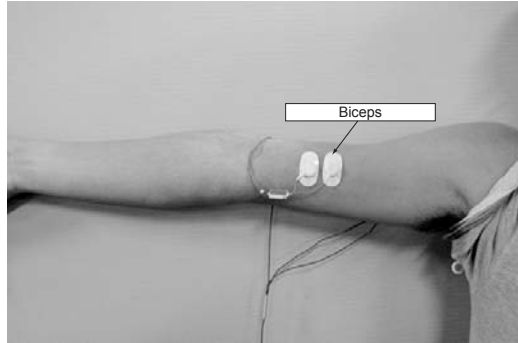
(b) Biceps (No.26)
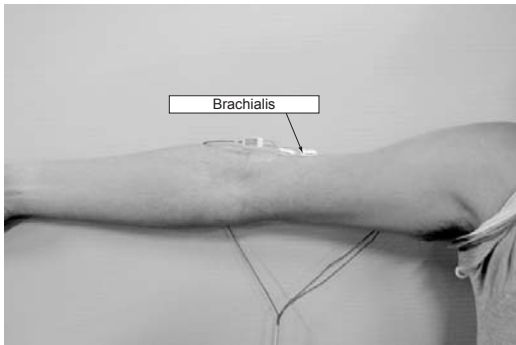
(c) Brachialis (No.27)

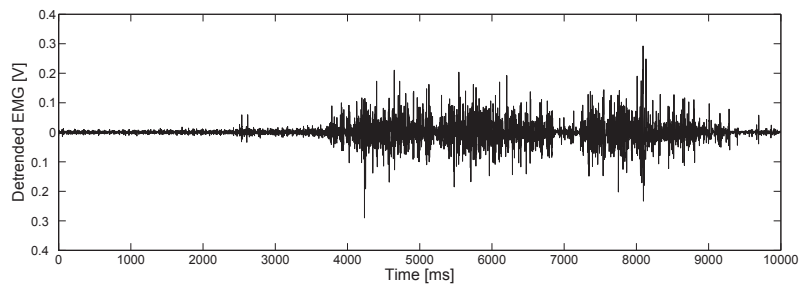(d) Brachioradials (No.28)

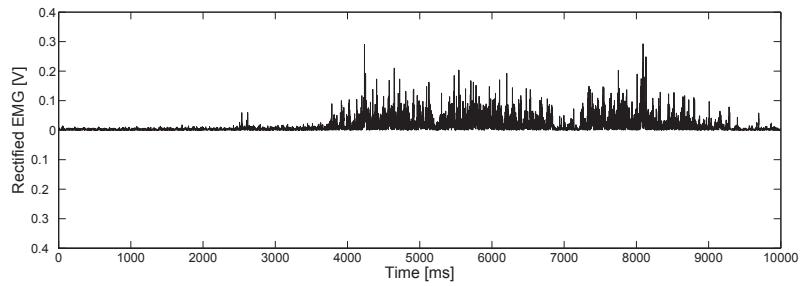(e) Flexor Carpi Ulnaris (No.33)

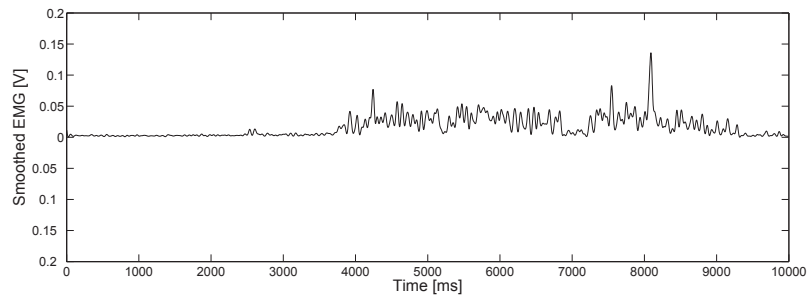Figure D.1. EMG signal measurement position

77

(a) Raw EMG signal

(b) Detrended EMG signal

(c) Rectified EMG signal

(d) Low-passed EMG signal

Figure D.2. Surface EMG signal processing

D.3 EMG signal and Muscle force

In this research, EMG signal is used to measure the change of muscle force with and without assist. In the past research, it has been confirmed that the EMG signal has a close relationship with muscle force. EMG signal and muscle force have the same change tendency. Muscle force f can be estimated from EMG signal using the following linear relation.

$$f = \sigma \cdot S \cdot \text{EMG} \cdot c, \tag{D.1}$$

where σ is the specific tension of muscle tissue for maximum muscle activation, S is the physiological cross-sectional area of muscle, EMG is the EMG signal, normalized to maximum voluntary contraction, and c is a factor for transforming relative EMG into relative muscle force [36]. For a linear EMG/force relationship, this factor is 1. For isometric movement, σ is constant and the change rate of EMG is the same as muscle force f. Therefore, in this research the change rate was compared with muscle force directly.
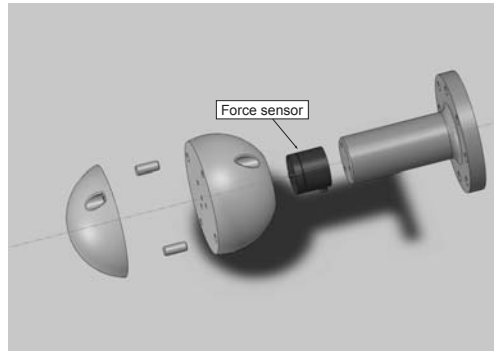
E. Construction of the handle
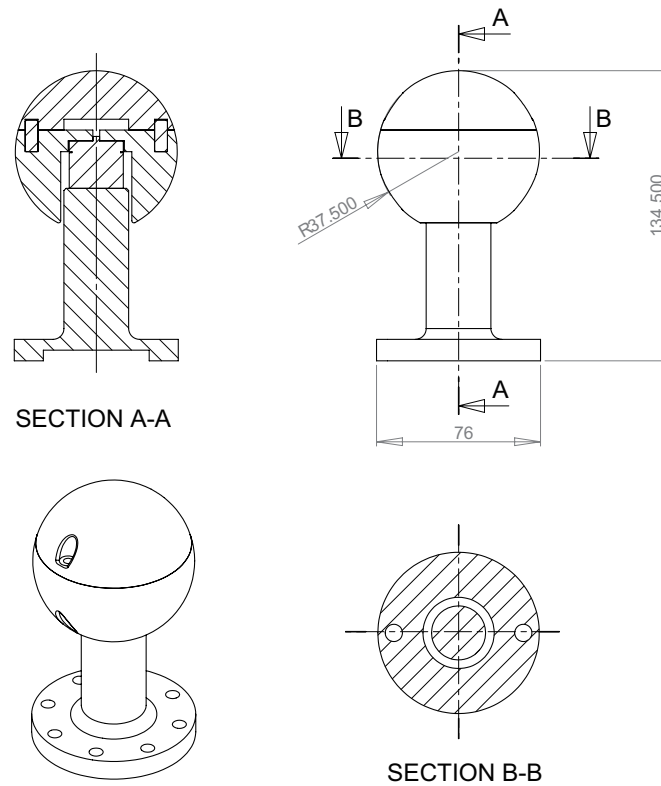

Figure E.1. Exploded view of handle

SECTION A-A

134.500

R37.500

76

SECTION B-B

Figure E.2. Drawing of handle

List of Publications

- Refereed Journal Papers -

1. **Ming Ding**, Jun Ueda and Tsukasa Ogasawara, "Pinpointed Muscle Force Control Using a Power-assisting Device", *Journal of the Robotics Society of Japan*, Vol. 27, No. 9, pp. 75-83, 2009 (in Japanese).

2. Shinji Kuriyama, **Ming Ding**, Yuichi Kurita, Jun Ueda and Tsukasa Ogasawara, "Flexible Sensor for McKibben Pneumatic Artificial Muscle", *International Journal of Automation Technology*, Vol. 3, No. 6, pp. 713-740, 2009.

- Refereed International Conference Proceedings Papers -

1. Jun Ueda, Moiz Hyderabadwala, **Ming Ding**, Tsukasa Ogasawara, Vijaya Krishnamoorthy and Minoru Shinohara, "Individual Muscle Control using an Exoskeleton Robot for Muscle Function Testing", *the 2009 Dynamic Systems and Control Conference (DSCC'09)*, October 12-14, Hollywood, California, 2009.

2. Shinji Kuriyama, **Ming Ding**, Yuichi Kurita, Jun Ueda, Tsukasa Ogasawara, "Flexible Sensor for Mckibben Pneumatic Actuator", *the 2009 IEEE Sensors Conference*, October 25-28, Christchurch, New Zealand, 2009.

3. **Ming Ding**, Jun Ueda and Tsukasa Ogasawara, "Pinpointed Muscle Force Control Using a Power-Assisting Device: System Configuration and Experiment", *the 2nd IEEE / RAS-EMBS International Conference on Biomedical Robotics and Biomechatronics (BioRob 2008)*, October 19-22, Scottsdate, USA, 2008.

4. **Ming Ding**, Jun Ueda and Tsukasa Ogasawara, "Development of MAS - a system for pin-pointed muscle force control using a power-assisting device", *the 2007 IEEE International Conference on Robotics and Biomimetics (Robio2007)*, December 15-18, Sanya, China, 2007.

5. Jun Ueda, **Ming Ding**, Masayuki Matsugashita, Reishi Oya and Tsukasa Ogasawara, ""Pinpointed control of muscles by using power-assisting device", *the 2007 IEEE International Conference on Robotics and Automation (ICRA 2007)*, pp. 3821-3828, Roma, Italy, April, 2007.

- Japanese Conference Proceedings Papers -

1. **Ming Ding**, Kotaro Hirasawa, Yuichi Kurita, Jun Ueda and Tsukasa Ogasawara, "Pinpointed Muscle Force Control: Comparison of Control Force Calculation Methods for Realizing Desired Muscle Force", *the 15th Robotics Symposia*, 2010.3.15-16.

2. **Ming Ding**, Yuichi Kurita, Jun Ueda, and Tsukasa Ogasawara, "Pinpointed Muscle Force Control Taking Into Account the DOF of Power-assisting Device", *the 27th Annual Conference of the Robotics Society of Japan*, AC1C3-03, 2009.9.15-17.

3. Kotaro Hirasawa, **Ming Ding**, Yuichi Kurita, and Tsukasa Ogasawara, "Pinpointed Muscle Force Control Considering the Human Posture and External Force", *the 27th Annual Conference of the Robotics Society of Japan*, AC1C3-04, 2009.9.15-17.

4. Shinji Kuriyama, **Ming Ding**, Yuichi Kurita, Jun Ueda, and Tsukasa Ogasawara, "State Observer for McKibben Actuator with Flexible Displacement Sensor", *the 9th Annual Conference of SICE System Integration Division of Japan (SI2008)*, 1G3-4, pp297-298, 2008.12.5-7.

5. Daisuke Nakamura, **Ming Ding**, Jun Ueda, and Tsukasa Ogasawara, "Posture estimation of a power-assisting device based on condition measurement of pneumatic rubber actuators", *the 11th Symposium on Construction Robotics in Japan (11th SCR)*, pp87-92, 2008.11.2.

6. Shinji Kuriyama, **Ming Ding**, Yuichi Kurita, Jun Ueda, Yoshio Matsumoto, and Tsukasa Ogasawara, "Axial Displacement Estimation of McKibben Actuator using Flexible Sensor", *the Robotics and Mechatronics Conference 2008(ROBOMEC2008)*, 1A1-C04, 2008.6.6-7.

7. Wataru Mori, **Ming Ding**, Yuichi Kurita, Jun Ueda, Yoshio Matsumoto, and Tsukasa Ogasawara, "Robot Hand Pitching Considering Contact Model Between Finger And Ball", *the 8th Annual Conference of SICE System Integration Divsion of Japan (SI2007)*, pp.695-696, 2007.12.20-22.

8. Satoru Uera, **Ming Ding**, Yuichi Kurita, Jun Ueda, and Tsukasa Ogasawara, "Analysis of interaction between power-assisting device and assisted muscle", *the 8th Annual Conference of SICE System Integration Divsion of Japan (SI2007)*, pp.1206-1207, 2007.12.20-22.

9. **Ming Ding**, Jun Ueda, and Tsukasa Ogasawara, "Feasibility of pinpointed muscle force control using a power-assisting device", *Welfare Engineering Symposium 2007*, pp.131-132, 2007.10.1-3.

10. **Ming Ding**, Jun Ueda, and Tsukasa Ogasawara, "Development of MAS — a software for pin-pointed muscle force control using a power-assisting device", *the 25th Annual Conference of the Robotics Society of Japan*, 3J34, 2007.9.13-15.

11. **Ming Ding**, Masahiro Kondo, Jun Ueda, Yoshio Matsumoto, and Tsukasa Ogasawara, "Pinpointed muscle force control using a power-assisting device", *the Robotics and Mechatronics Conference 2007(ROBOMEC2007)*, 2A2-C09, 2007.5.11-12.

12. **Ming Ding**, Masahiro Kondo, Jun Ueda, Yoshio Matsumoto, and Tsukasa Ogasawara, "Force Display Method with Muscle Force Control Utilizing Muscle/Articial-Muscle Integrated Human Model", *the Robotics and Mechatronics Conference 2006(ROBOMEC2006)*, 1P1-D07, 2006.5.26-28.

- Tutorial -

1. Tsukasa Ogasawara, **Ming Ding**, and Jun Ueda, "Development of Movement Function Assist Device and Muscle Force Control During Movements", *Science and Industry*, Vol. 83, No. 10, pp. 9–17, 2009 (in Japanese).

- Patents -

1. Jun ueda, Tsukasa Ogasawara, and **Ming Ding**, "Driving force calculating device, driving force calculating method, power", *USA Patent 7529632*, 2009.